

# A Comprehensive Database of Thawing Permafrost Locations Across Alaska: **Version 2.0.0**

Hailey Webb<sup>1,2</sup>, Ethan Pierce<sup>3</sup>, Benjamin W. Abbott<sup>4</sup>, William B. Bowden<sup>5</sup>, Yaping Chen<sup>6</sup>, Yating Chen<sup>7</sup>, Thomas A. Douglas<sup>8</sup>, Joel F. Eklof<sup>9,10</sup>, Eugénie S. Euskirchen<sup>11</sup>, Moritz Langer<sup>12,13</sup>, Isla H. Myers-Smith<sup>14</sup>, Irina Overeem<sup>15</sup>, Jens Strauss<sup>13</sup>, Katey Walter Anthony<sup>16</sup>, Kang Wang<sup>17</sup>, Matthew A. Whitley<sup>18</sup>, Merritt R. Turetsky<sup>1,2</sup>

<sup>1</sup>Renewable and Sustainable Energy Institute, University of Colorado Boulder, Boulder, CO 80303, USA

<sup>2</sup>Ecology and Evolutionary Biology, University of Colorado Boulder, Boulder, CO 80302, USA

<sup>3</sup>Thayer School of Engineering, Dartmouth College, Hanover, ~~NH~~ 03755, USA

<sup>4</sup>Department of Plant & Wildlife Sciences, Brigham Young University, Provo, UT USA

<sup>5</sup>Rubenstein School of Environment and Natural Resources, University of Vermont, Burlington, VT USA 05401

<sup>6</sup>School of Ecology, Sun Yat-sen University, Shenzhen 518107, China

<sup>7</sup>College of Geography and Environment, Shandong Normal University, Jinan, 250014, China

<sup>8</sup>U.S. Army Cold Regions Research and Engineering Laboratory, Fort Wainwright, AK 99703 USA

<sup>9</sup>Department of Environmental Studies and Sciences, University of Puget Sound, Tacoma, WA, USA 98416

<sup>10</sup>Department of Civil and Environmental Engineering, University of Washington, Seattle, WA USA 98195

<sup>11</sup>Institute of Arctic Biology, University of Alaska Fairbanks, Fairbanks, AK 99775 USA

<sup>12</sup>Department of Earth Sciences, Vrije Universiteit Amsterdam, De Boelelaan 1085, 1081HV Amsterdam, the Netherlands

<sup>13</sup>Alfred Wegener Institute Helmholtz Centre for Polar and Marine Research, Permafrost Research Section, 14473 Potsdam, Germany

<sup>14</sup>Department of Forest & Conservation Sciences, Faculty of Forestry, University of British Columbia, Vancouver, British Columbia, Canada V6T 1Z4

<sup>15</sup>Institute of Arctic and Alpine Research, University of Colorado Boulder, Boulder, CO 80303, USA

<sup>16</sup>Water and Environmental Research Center, University of Alaska Fairbanks, Fairbanks, AK 99775 USA

<sup>17</sup>School of Geographic Sciences, East China Normal University, Shanghai 200241, People's Republic of China

<sup>18</sup>Little Place Labs Ltd, 128 City Road, London EC1V 2NX, United Kingdom

Correspondence to: Hailey Webb ([hailey.webb@colorado.edu](mailto:hailey.webb@colorado.edu))

**Abstract.** The Arctic is warming nearly four times faster than the global average, leading to widespread permafrost thaw degradation with profound implications for ecosystems, ~~and infrastructure~~. While gradual permafrost thaw occurs over decades, abrupt thaw events - such as thermokarst formation or retrogressive thaw slumps - can rapidly alter ecosystems and severely damage infrastructure. Although abrupt thaw is increasingly widespread, comprehensive datasets that map its spatial distribution at regional scales for land managers and local governments are still lacking. To address this gap, we created the Alaska Permafrost Thaw Database, an open-access, collaborative database which compiles 19,540 permafrost thaw and thermokarst locations across Alaska from 44 sources, integrating field observations, remote sensing products, and the published literature. This database spans observations from 1950 through ~~the~~ present and incorporates datasets of varying spatial resolution, ranging from field-based point measurements to remotely sensed products (1-125 m), providing statewide coverage across Alaska. The dataset includes abrupt thaw features and sites experiencing gradual top-down thaw that can help to support comparative analysis and predictive modeling. We used this database to explore relationships between thaw type (abrupt vs. non-abrupt) and topographic metrics (i.e., slope, relative elevation, and potential incoming solar radiation), analyze the distribution of various thaw features across Alaska's major ecoregions, and compare the database to current spatial datasets of ground ice and Yedoma. Our analysis shows abrupt thaw features are more prevalent in lowlands and depressions while gradual top-down and lateral thaw features are more commonly associated with areas receiving higher potential incoming solar radiation such as south facing slopes and open clearings. We also found substantial mismatches between ice-driven thaw processes and existing ground ice and Yedoma maps, likely reflecting the coarse resolution of current mapping products relative to the fine-scale nature of field measurements and highlighting the limitations of current datasets for local-scale prediction. The database provides direct, empirical evidence of actively thawing and stable permafrost locations and can be used to inform and validate ground ice mapping. By comparing the database with physiographic characteristics and remotely sensed measurements, the database can guide future field campaigns in areas with little to no observations. As permafrost thaw transforms Arctic landscapes, high-resolution, accessible spatial data - such as our thaw database - will be critical for informing ~~mitigation~~ and adaptation strategies. The Alaska Permafrost Thaw Database is openly available at Zenodo (<https://doi.org/10.5281/zenodo.16996415>), which provides a link to the GitHub repository and access to all versions; this paper describes version 2.0.0.

Deleted: MA

Deleted: ,

Deleted: , and global climate feedbacks

Deleted: climate

56 **1 Introduction**

57 The Arctic is one of the most rapidly changing environments on Earth (Ballinger et al., 2025). Ongoing widespread permafrost  
58 thaw, increased wildfire activity, changes in snowfall and precipitation, and sea level rise are all disrupting Indigenous and local  
59 communities and affecting infrastructure (Bamber et al., 2019; Bigalke and Walsh, 2022; Hjort et al., 2022; McCarty et al., 2021;  
60 Stepien et al., 2014; Streletskiy et al., 2023; Vincent, 2020). Permafrost underlies approximately 80% of the land surface in  
61 Alaska and serves as a critical component of the state’s ecosystems, landscape stability, hydrology, and carbon dynamics  
62 (Andresen et al., 2020; Jorgenson et al., 2006; Schuur et al., 2015). Terrestrial permafrost stores at least two times the amount of  
63 carbon currently in the atmosphere (between 1,460 - 1,600 Gt) (Schuur et al., 2022; Strauss et al., 2025). When permafrost  
64 thaws, microorganisms partially decompose soil carbon and release it in the form of greenhouse gases including carbon dioxide  
65 and methane (Mackelprang et al., 2016).

66  
67 Abrupt permafrost thaw could impact up to 20% of the permafrost region (Olefeldt et al., 2016). Unlike gradual thaw, which  
68 occurs when the active layer thickens by a few centimeters a year and causes a gradual shift in vegetation and slower, sustained  
69 shift in the carbon balance (Harris et al., 1988), abrupt thaw processes initiate within a few decades and cause severe impacts on  
70 the surrounding ecosystem (Turetsky et al., 2019; Webb et al., 2025a). Many abrupt thaw processes are triggered by the melting  
71 of ground ice, but not all forms of abrupt thaw depend on high ground ice to occur (i.e., coastal erosion, wildfire-induced top-  
72 down thaw) (Webb et al. 2025a). In upland and/or sloped regions, abrupt thaw can manifest as, for example, thaw slumps and  
73 active layer detachments while collapse scar wetlands and thermokarst lakes form in more poorly drained lowlands (Olefeldt et  
74 al., 2016; Turetsky et al., 2020). These processes are especially pronounced in regions underlain by Yedoma - ice-rich  
75 Pleistocene-aged permafrost containing large ice wedges (Strauss et al., 2021) - where thawing drives ground subsidence and  
76 exposes large stores of previously frozen, bioavailable carbon. Besides the impact of abrupt thaw on ecosystem structure and  
77 carbon cycling, abrupt thaw events also pose significant threats to infrastructure (Hjort et al., 2022). In Alaska, maintaining and  
78 rebuilding infrastructure damaged by permafrost thaw is expected to cost between \$14.2–24.5 billion by 2050 (Streletskiy et al.,  
79 2023). Understanding the spatial distribution of permafrost thaw events is essential for predicting future permafrost degradation  
80 and informing mitigation strategies.

81  
82 Despite the increasing occurrence of abrupt thaw events, comprehensive datasets documenting their spatial distribution are  
83 limited. Existing datasets either focus on specific regions (Jones and Zuck, 2016; Nitze et al., 2020b; Swanson, 2021; Whitley et  
84 al., 2018) or, if pan-Arctic, are limited to a single type of abrupt thaw such as retrogressive thaw slumps (Olefeldt et al., 2016;  
85 Yang et al., 2025). In Alaska, datasets contain too few thaw features to support robust modeling and often rely on automated  
86 methods that are less reliable than direct field observations (Witharana et al., 2022; Yang et al., 2023). To address this gap, we  
87 compiled a dataset of 19,540 permafrost thaw and thermokarst occurrences across Alaska from 44 different sources. This dataset  
88 includes various abrupt thaw features (i.e., thermokarst lakes, retrogressive thaw slumps, thermokarst wetlands) as well as  
89 locations that are not experiencing abrupt thaw that represent areas of more stable permafrost or permafrost subject to gradual  
90 top-down thaw. These so-called “non-abrupt thaw features” were compiled from a combination of permafrost monitoring  
91 networks, active layer depth surveys, and photo-interpretations of landscape change through time. These sites represent gradual  
92 thaw processes and are located in areas distinct from abrupt thaw features, allowing them to be treated as independent  
93 observations. These non-abrupt thaw locations serve as control points for comparison and provide a valuable reference for  
94 modeling permafrost dynamics, helping to distinguish the environmental conditions associated with abrupt thaw from those  
95 where thaw may be occurring more gradually or not at all. While the absence of visible abrupt thaw does not guarantee low risk,  
96 these locations could represent potential locations for infrastructure development and provide insights into the physiographic  
97 characteristics of permafrost more stable to change than abrupt thaw locations.

98  
99 In this study, we carried out an extensive search of peer-reviewed literature, published datasets, and unpublished field  
100 observations to assemble the most comprehensive database of permafrost thaw locations across Alaska to date. We use the  
101 database to analyze topographic differences between abrupt and non-abrupt thaw sites, including slope, relative elevation, and  
102 potential incoming solar radiation. We also evaluate the ability of current ground ice maps to capture fine-scale susceptibility to  
103 ice-dependent abrupt thaw processes and quantify the proportion of these processes that occur within the Yedoma domain. This  
104 study represents the first large-scale, field-based comparison of mapped ground ice distributions with observed thaw features,  
105 assessing the ability of these maps to reliably predict abrupt thaw vulnerability. Specifically, we compare ice-dependent abrupt  
106 thaw features with the widely used ground ice map for Alaska developed by Jorgenson et al. (2008), the circumpolar ground ice  
107 map by Heginbottom et al. (2002) and the Database of Ice-Rich Yedoma Permafrost by Strauss et al. (2022). By comparing  
108 observed thaw features with mapped ground ice, Yedoma distribution, and topographic variables, we aim to assess current model  
109 limitations and identify key environmental characteristics associated with abrupt thaw across Alaska. These insights can help  
110 refine permafrost hazard assessments and guide the development of more accurate predictive tools for abrupt thaw formation and  
111 adaptation planning.

**Deleted:** Anthropogenic climate change is projected to raise the average global temperature by 2-4.9 °C by the end of the 21st century (Raftery et al., 2017). However, warming is not uniform across the planet and the Arctic is warming nearly four times faster than the global average, making it one of the most rapidly changing environments on Earth (Rantanen et al., 2022). Climate change in Arctic and sub-Arctic regions is causing widespread permafrost thaw, increased wildfire activity, changes in snowfall and precipitation, and sea level rise, all of which disrupt Indigenous and local communities and affect infrastructure (Bamber et al., 2019; Bigalke and Walsh, 2022; Hjort et al., 2022; McCarty et al., 2021; Stepien et al., 2014; Streletskiy et al., 2023; Vincent, 2020). Permafrost underlies approximately 80% of the land surface in Alaska and serves as a critical component of the state’s ecosystems, landscape stability, hydrology, and carbon dynamics (Andresen et al., 2020; Jorgenson et al., 2006; Schuur et al., 2015). Terrestrial permafrost stores at least two times the amount of carbon currently in the atmosphere (between 1,460 - 1,600 Gt) making its warming and thaw a major concern for global climate feedbacks (Schuur et al., 2022; Strauss et al., 2025). When permafrost thaws, microorganisms partially decompose soil carbon and release it in the form of greenhouse gases including carbon dioxide and methane that can accelerate climate change (Mackelprang et al., 2016).¶

**Deleted:** (Olefeldt et al., 2016). Unlike gradual thaw, which occurs when the active layer thickens by a few centimeters a year...

**Deleted:** In upland and/or sloped regions, abrupt thaw can manifest as, for example, thaw slumps and active layer detachments while collapse scar wetlands and thermokarst lakes form in more poorly drained lowlands (Olefeldt et al., 2016; Turetsky et al., 2020)

**Deleted:** depending on future climate warming trajectories

**Deleted:** are broadly representative of

**Deleted:** across Alaska

**Deleted:** climate

151 **2 Methods**

152 **2.1 Data Sources and Consolidation Methods**

153 We compiled the database from a combination of ground-truthed field observations and remotely sensed data across Alaska.  
 154 Table 1 provides a summary of the sources used to extract thaw occurrence locations. We sourced these locations from a variety  
 155 of formats including geospatial databases, coordinates reported in published journal articles, field campaigns, and photo-  
 156 interpreted sites of landscape change. Given that spatial datasets were often in different formats such as points, polylines, and  
 157 polygons, we standardized the database by converting all locations to point features, based on the centroid of the feature  
 158 (polygons) or the midpoint of the line (polylines).  
 159

Deleted: .

Authors	Data Source Type	Imagery Used	Imagery Dates	Imagery Resolution (meters)	Number of Features	Types of Features
(Abbott and Jones, 2013)	Field - published				93	Active layer detachment, Thermoerosional gully, Retrogressive thaw slump
(Balsler and Jorgenson, 2013)	Field - published				35	Active layer detachment, Retrogressive thaw slump, Thermoerosional gully, Thermokarst
(Bowden et al., 2008)	Field - published				32	Retrogressive thaw slump, Thermoerosional gully, Thermokarst
(Buckeridge et al., 2013, 2023)	Field - published				3	Retrogressive thaw slump
(Chen et al., 2021b)	Remote sensing - published	Commercial satellite images	1950 through 2015	~1	216	Thermokarst, Wildfire-induced thaw
(Chen et al., 2021a)	Remote sensing - published	Landsat TM, ETM+, and OLI	2000 through 2020	30	90	Thermokarst lake
(Douglas et al., 2021)	Field - published				3	Thermokarst
(Douglas, Thomas)	Field - unpublished				13	Thermokarst
(Edwards et al., 2016)	Field - published				3	Thermokarst lake

Formatted Table

(Euskirchen et al., 2014)	Field - published				1	Thermokarst wetland
(GTN-P, 2015a)	Field - published				65	Non-abrupt
(GTN-P, 2015b)	Field - published				172	Non-abrupt
(Gooseff, 2016)	Field - published				456	Thaw pond, Thermokarst, Thermokarst lake, Wildfire-induced thaw
(Harms et al., 2013)	Field - published				3	Thermoerosional gully, Thermokarst
(Hinkel et al., 2012)	Field - published				28	Thermokarst lake
(Hopkins, 1949)	Field - published				1	Thermokarst lake
(Johnston et al., 2014)	Field - published				14	Non-abrupt, Thermokarst wetland
(Jones and Zuck, 2016)	Remote sensing - published	SAR; Landsat TM; ETM+; OLI	1985 through 2015	30	3542	Thermokarst lake, Thaw pond
(Jones et al., 2013)	Field - published				1	Thermokarst wetland
(Jones et al., 2016)	Field - published				1	Thermokarst wetland
(Jones et al., 2019)	Remote sensing/Photo-interpretation - published	USGS topo maps; aerial photography ; Landsat TM; ETM+; OLI	2000 through 2017	30	74	Thermokarst lake
(Jones et al., 2023)	Field - published				1	Thermokarst lake
(Jongejans et al., 2018)	Field - published				4	Thermokarst lake
(Jorgenson, 2013)	Field - published				49	Active layer detachment, Retrogressive thaw slump, Thermoerosional gully,

						Thermokarst, Wildfire-induced thaw
(Jorgenson et al., 2022)	Remote sensing/photo-interpretation - published		Photo-interpretation		800	Non-abrupt, Retrogressive thaw slump, Thermoerosional gully, Thermokarst, Thermokarst wetland
(Kallio and Rieger, 1969)	Field - published				1	Thermokarst
(Klein et al., 2013)	Field - published				1	Thermokarst
(Langer et al., 2020)	Field - published				10	Thermokarst lake
(Lenz et al., 2016)	Field - published				3	Thermokarst lake
(Liljedahl et al., 2007)	Field - published				1	Wildfire-induced thaw
(Lloyd et al., 2003)	Field - published				1	Thaw pond
(Luken and Billings, 1984)	Field - published				1	Thermokarst
(Myers-Smith et al., 2007)	Field - published				1	Thermokarst
(Myers-Smith et al., 2008)	Field - published				1	Thermokarst
(Nitze et al., 2018)	Remote sensing - published	Landsat	1999 through 2014	30	194	Retrogressive thaw slump
(Nitze et al., 2020a)	Remote sensing - published	Landsat; Sentinel-1; PlanetScope	1999 through 2018	30; 3.125	6555	Thermokarst lake
(Osterkamp et al., 2018)	Field - published				1	Thermokarst
(Plug and West, 2009)	Field - published				2	Thermokarst lake
(Strauss et al., 2022)	Field - published				1	Thermokarst lake

(Swanson, 2021)	Remote sensing - published	Alaska high altitude aerial photographs ; IKONOS; SPOT67; WV23	1977 through 2015	1.5; 4; 2.2; 6	6574	Active layer detachment, Retrogressive thaw slump
(Turetsky et al.)	Field - unpublished				104	Non-abrupt, Thaw pond, Thermoerosional gully, Thermokarst, Thermokarst lake, Thermokarst wetland
(Walter Anthony, 2020)	Field - published				16	Thermokarst lake
(Wang et al., 2018a, b)	Field - published				47	Non-abrupt
(Whitley et al., 2018)	Field - published				326	Non-abrupt, Thermoerosional gully, Thermokarst

**Table 1.** Summary and descriptions of the published sources used to create the thaw database.

Each of these sources employed different data collection methods resulting in varying levels of accuracy in their final outputs. In particular, the spatial and temporal resolution of remote sensing data has improved significantly over time. Older studies often relied on moderate-resolution imagery such as Landsat (30 meters), while more recent measurements frequently utilize high-resolution datasets like ArcticDEM (2 meters), enabling more precise detection and characterization of thaw features. We did not manually verify each individual feature, and the features in the database reflect the accuracy of their source dataset. While a comprehensive and quantitative statistical uncertainty analysis is not possible due to the heterogeneity and lack of validation data for our input sources, we have provided metadata on source type, satellite(s) or sensor(s) used (if remotely sensed data), data year(s), and spatial resolution. This level of documentation allows the reliability and limitations of the dataset to be evaluated transparently by users. In addition, the open-access and collaborative nature of the database enables community feedback including the identification and correction of errors, duplicates, omissions, or regional gaps, and provides clear opportunities for continued refinement and expansion as new data become available. To increase consistency across sources, we applied several post-processing techniques to improve data quality (Table 2). These methods included filtering out points located outside the zone of mapped permafrost in Alaska, using only the most recent thaw data when multiple years of thaw data was presented from each source, and removing duplicate locations. Duplicate entries of thaw features with identical names were removed, keeping only the first occurrence of each named feature. For example, both Wang et al. (2018a,b) and the Global Terrestrial Network for Permafrost included sites from the Circumpolar Active Layer Monitoring Network (CALM).

Source	Data Selection Criteria and Methods
(Jones and Zuck, 2016)	<ul style="list-style-type: none"> <li>Selected lakes that were classified as remnant drained lake basins, primary or secondary thermokarst or depression lakes, and collapsed pingo ponds.</li> <li>Total lakes removed = 820</li> </ul>
(Jones et al., 2019)	<ul style="list-style-type: none"> <li>Removed lakes that were drained by mechanisms caused by humans, coastal erosion, or river meandering</li> <li>Total lakes removed = 24</li> </ul>
(Jorgenson et al., 2022)	<ul style="list-style-type: none"> <li>Used the ecosystem shift change code between 1950-2020 to classify each location as abrupt or non-abrupt thaw.</li> </ul>

- Deleted:** Rather than
- Deleted:** verifying
- Deleted:** thaw
- Deleted:** we assume that
- Deleted:** reflects
- Deleted:** the original sources
- Deleted:** lacking
- Deleted:** of
- Deleted:** This transparency, combined with ongoing opportunities for community feedback, is an effective means of ensuring reliability and continued improvement of the database....
- Formatted Table**
- Formatted:** Indent: Hanging: 0.19"
- Formatted:** Indent: Hanging: 0.2"
- Formatted:** Indent: Hanging: 0.18"

	<ul style="list-style-type: none"> <li>No locations were removed</li> </ul>
(Nitze et al., 2018)	<ul style="list-style-type: none"> <li>Only used points from the RTS (Retrogressive thaw slump) data file</li> </ul>
(Nitze et al., 2020a)	<ul style="list-style-type: none"> <li>Removed duplicate lakes between Planet and Landsat/S1 imagery</li> <li>Total lakes removed = 4,124</li> </ul>
(Swanson, 2021)	<ul style="list-style-type: none"> <li>Removed duplicate features across the various satellites and remote sensors used</li> <li>Total features removed = 383</li> </ul>
(Whitley et al., 2018)	<ul style="list-style-type: none"> <li>Removed locations that: <ul style="list-style-type: none"> <li>Had no permafrost</li> <li>Were classified as water or wrack line</li> </ul> </li> <li>Total features removed = 167</li> </ul>

**Table 2.** Description of post-processing methods applied to the relevant database sources. If a source from Table 1 is not listed here, it indicates that no additional quality control measures were needed for the data.

For each point feature, we recorded the identifying source information (authors, DOI), the type of source (field or remote sensing) and its publication status, feature name (if applicable), latitude and longitude (in WGS 84), feature type as reported by the source (i.e., retrogressive thaw slump, thermokarst fen), feature category (feature type simplified into a broader category), type of thaw (abrupt or non-abrupt), and the imagery used along with relevant mapping information such as imagery dates and resolution. Table 3 details these attributes and Table 4 defines the thaw feature categories used in our database. We classified features as abrupt or non-abrupt thaw according to the framework outlined in Webb et al. (2025a), specifically using the decision tree in Figure 5. Under this scheme, a thaw event is considered abrupt if it develops within 30 years and meets at least one of the following criteria: it involves substrate with high ground ice content (>20 %) or it results in a major ecosystem impact, even in the absence of high ground ice. ~~All other features were classified as non-abrupt.~~

Field Name	Format	Description
Authors	Author last name et al. (year published)	Author list from source publication
DOI	https://doi.org/XXXX/XXXX	Unique identifier from source publication. N/A if unpublished data
DataSourceType	Must be one of the following or a combination: <ul style="list-style-type: none"> <li>Field - published/unpublished</li> <li>Remote sensing - published/unpublished</li> <li>Photo interpretation - published/unpublished</li> </ul>	The type of source data and publication status. This can include field observations, remotely sensed data, or photo-interpreted data
FeatureName	Name of feature or site	The name of the feature. This can include lakes, monitoring stations, established field sites, etc. Leave blank if there is no name.
Latitude	Decimal Degrees	Point location (y coordinate) of thaw event in EPSG:4326
Longitude	Decimal Degrees	Point location (x coordinate) of thaw event in EPSG:4326
FeatureType	Type of feature as reported by source data	The type of feature as reported by the source data. This can include things like retrogressive thaw slumps, thermokarst lakes, collapse-scar bog, etc.
FeatureCategory	Must be one of the following: <ul style="list-style-type: none"> <li>Active layer detachment</li> <li>Retrogressive thaw slump</li> <li>Thaw pond</li> <li>Thermoerosional gully</li> <li>Thermokarst</li> <li>Thermokarst lake</li> </ul>	FeatureType generalized into broader category

Formatted: Indent: Hanging: 0.2"

Formatted: Indent: Hanging: 0.2"

Formatted: Indent: Hanging: 0.2"

Formatted: Indent: Hanging: 0.18"

Formatted: Indent: Hanging: 0.2"

**Deleted:** We chose not to classify non-abrupt features as gradual thaw because this implies that thaw is occurring at these locations. While this may be true for a majority of the permafrost region, it would be wrong to assume this is the case for all areas.

Formatted Table

	<ul style="list-style-type: none"> <li>● Thermokarst wetland</li> <li>● Wildfire-induced thaw</li> <li>● Non-abrupt</li> </ul>	
ThawType	Must be one of the following: <ul style="list-style-type: none"> <li>● Abrupt</li> <li>● Non-abrupt</li> </ul>	The type of thaw. The features are classified as either abrupt or non-abrupt thaw according to the framework outlined in Webb et al. (2025a).
Imagery	Remote sensing instrument(s) used	For remotely sensed data, record the instrument(s) used to map thaw features. This can be the name of a satellite, aerial campaign, drone imagery, etc.
ImageryDates	Date of imagery used	For remotely sensed data, include the date range of imagery used
ImageryResolution_meters	Resolution of imagery	For remotely sensed data, include the spatial resolution, in meters, of the mapped thaw features

**Table 3.** Attributes recorded for each point feature in the database including units (when relevant) and descriptions of variables.

Thaw Feature	Definition	Requires high ground ice?
Active layer detachment	A landslide in which the thawed surface layer of the ground detaches and slides downslope over frozen soil	No
Retrogressive thaw slump	A bowl-shaped landslide in ice-rich permafrost that enlarges each summer as exposed ground ice melts and headwall collapses	Yes
Thaw pond	A small waterbody that forms when ice-rich permafrost thaws and subsides, creating surface depressions that fill with trapped meltwater, snowmelt, or precipitation	Yes
Thermoerosional gully	A process in polygonal networks initiated by the infiltration of runoff water (e.g. snowmelt, rainfall) into open cracks and cavities in the active layer which can develop over a single thawing season	Yes
Thermokarst	Process by which characteristic landforms result from the thawing of ice-rich permafrost or the melting of massive ice	Yes
Thermokarst lake	A lake formed or affected by the thaw of ice-rich permafrost	Yes
Thermokarst wetland	The collapse of ice- and peat-rich soils on a flat landscape	Yes
Wildfire-induced thaw	When wildfire removes insulating vegetation and organic soil layers, increases surface albedo and ground heat flux, and alters hydrology, accelerating permafrost thawing	No
Non-abrupt	A feature where the thaw front progresses slowly over several years to decades, has low or no ground ice, and does not have a substantial impact to the ecosystem	Never

Formatted Table

Deleted: thaw

Deleted: that takes longer than 30

Deleted: emerge

**Table 4.** Definitions for the major permafrost thaw categories in the thaw database. Definitions for features were derived from (Gagnon et al., 2024; Gibson et al., 2018; Lewkowicz et al., 2024; Li et al., 2017; National Snow and Ice Data Center (NSIDC), n.d.; Wendel, 2016; Yoshikawa et al., 2002).

## 2.2 Ecoregion Classification

We divided Alaska into ecoregions based on the EPA’s Level III Ecoregions map (U.S. Environmental Protection Agency, 2012), using Level II classifications with some adjustments (Fig. 1). We distinguished the Brooks Range from the Arctic Tundra, grouped the southern mountain ranges together under a single “Southern Mountains” ecoregion, and classified all areas along the southern coast as “Maritime”. Then, we spatially joined the thaw database with the ecoregion map and quantified the occurrence of various abrupt thaw features within each unique ecoregion.

Deleted: Table 4. Definitions for the major permafrost thaw categories in the thaw database. Definitions for features were derived from (Gagnon et al., 2024; Gibson et al., 2018; Lewkowicz et al., 2024; Li et al., 2017; National Snow and Ice Data Center (NSIDC), n.d.; Wendel, 2016; Yoshikawa et al., 2002).  
**2.2 Ecoregion Classification**  
 We divided Alaska into ecoregions based on the EPA’s Level III Ecoregions map (U.S. Environmental Protection Agency, 2012)...

234 **2.3 Environmental Data Extraction**

235 To characterize terrain conditions at observed thaw features, we extracted high-resolution topographic variables from the  
236 ArcticDEM (V.4.1) (Porter et al., 2023) using Google Earth Engine (GEE) (Gorelick et al., 2017). We calculated elevation (m),  
237 slope (degrees), and aspect (degrees) using the terrain function in GEE. The terrain function derives slope in degrees using a 3x3  
238 pixel window around each point. Since the ArcticDEM has a spatial resolution of 2 m, slope was computed from a 36-m<sup>2</sup>  
239 neighborhood centered on each point. To quantify a thaw feature’s topographic position on the landscape, we computed relative  
240 elevation by subtracting the mean elevation within a 100-m circular neighborhood from the elevation at each thaw point (Eq. 1).  
241 This first-order approximation yields values less than 0 for depressions and values greater than 0 for elevated terrain.

Deleted: 6

$$h_{rel}(i) = h_i - \bar{h}_{S_i}$$

245  $h_{rel}(i)$  = Relative elevation  
246  $h_i$  = Elevation at point  $i$   
247  $\bar{h}_{S_i}$  = Mean elevation within a 100-m circular neighborhood around  $i$

(1)

251 We calculated a solar radiation index (SRI) following the methods outlined in (Fu and Rich, 2002) (Eq. 2). The SRI estimates the  
252 potential incoming solar radiation under clear-sky conditions at solar noon on the summer solstice (June 21). To define a  
253 representative solar azimuth angle for Alaska, we used the NOAA Solar Calculator and selected the geographic center of the  
254 state (64.73°N, 152.47°W) since solar azimuth varies minimally across Alaska that time of year. We approximated the solar  
255 zenith angle, which varies with latitude, by calculating the absolute difference between each thaw location’s latitude and solar  
256 declination on the solstice. We acknowledge that the SRI is a simplified proxy for solar energy input, and that local factors such  
257 as canopy cover, microclimate, and seasonal daylength variation also influence site-specific solar exposure. However, the SRI  
258 provides a useful estimate of potential solar energy input that may affect permafrost thaw vulnerability and is more informative  
259 than aspect alone. Because Alaska is at high latitude, the solar radiation index values are centered around ~0.75 for flat terrain,  
260 with higher values indicating steeper, south-facing slopes and lower values indicating north-facing slopes or less-exposed terrain.

$$SRI = \cos(\theta_z) \cos(\beta) + \sin(\theta_z) \sin(\beta) \cos(\phi - \alpha)$$

262  $\theta_z$  = solar zenith angle  
263  $\beta$  = slope  
264  $\phi$  = aspect  
265  $\alpha$  = solar azimuth angle

Deleted:  $SRI = \cos(\theta_z) \cos(\beta) + \sin(\theta_z) \sin(\beta) \cos(\theta_z)$

Deleted:  $\beta$

Deleted:  $\phi$

Deleted:  $\alpha$

(2)

269 To examine topographic variation in slope, relative elevation, and SRI between abrupt and non-abrupt thaw locations, we  
270 performed non-parametric Wilcoxon rank-sum tests (McKnight and Najab, 2010). Because the database is heavily skewed  
271 towards abrupt thaw features, we used a bootstrapping approach to balance sample sizes (Efron and Tibshirani, 1993). We  
272 conducted 1,000 iterations of stratified random sampling, selecting 500 abrupt thaw points and 500 non-abrupt thaw points with  
273 replacement in each iteration. We calculated 95 % confidence intervals for the mean values of each variable within abrupt and  
274 non-abrupt thaw groups based on the bootstrapped samples. All statistical analyses were conducted in R (version 4.5.0) and the  
275 associated code and results can be found at our GitHub repository: ([https://github.com/ArcticWebb/Alaska\\_Permafrost\\_Thaw\\_](https://github.com/ArcticWebb/Alaska_Permafrost_Thaw_Database)  
276 [Database](https://github.com/ArcticWebb/Alaska_Permafrost_Thaw_Database))

Deleted: .)

278 **2.4 Spatial Comparison with Ground Ice and Yedoma Maps**

279 Areas with high ground ice content are especially prone to abrupt permafrost thaw due to substantial volume loss when ice melts.  
280 Ground ice is widely recognized as one of the most influential factors driving abrupt thaw (Jorgenson et al., 2006; Teufel and  
281 Sushama, 2019; Turetsky et al., 2020) and many permafrost thaw prediction models use it as a key variable for identifying areas  
282 at risk. We acknowledge that precipitation, vegetation, snow cover, and other factors can also influence abrupt thaw, however,  
283 many of these drivers are indirectly represented in ground ice maps because those maps are developed using environmental  
284 indicators as model inputs. Existing ground ice maps for Alaska were produced at coarse spatial resolutions (statewide or  
285 circumpolar) which limits their utility for fine-scale mapping (Heginbottom et al., 2002; Karjalainen et al., 2022). For this study,

293 we compared two of the most widely used datasets: one developed specifically for Alaska and another designed for pan-Arctic  
294 ground ice conditions. The *Permafrost Characteristics of Alaska* map by Jorgenson et al. (2008) estimates ground ice content  
295 within the upper 20 meters of permafrost based on terrain originally described in Kreig and Reger (1982) and is supplemented  
296 with field observations. Inconsistent or patchy permafrost distribution is classified as variable, < 10 % as low, 10-40 % as  
297 moderate, and > 40 % as high. In contrast, the *Circum-Arctic Map of Permafrost and Ground-Ice Conditions, Version 2* by  
298 (Heginbottom et al., 2002) summarizes permafrost conditions and ground ice distribution across the Northern Hemisphere (20°N  
299 to 90°N). Ground ice classification is also based on the upper 20 meters of permafrost, with < 10 % defined as low, 10-20 % as  
300 moderate, and > 20 % as high. Because the two datasets use different percentage thresholds to define moderate and high ground  
301 ice content, we combined the moderate and high classes into a single category for each map while retaining low ground ice as a  
302 distinct class since both maps define it as < 10 %. This approach groups the majority of landscapes where abrupt thaw is  
303 considered probable or highly likely (moderate or high ground ice) while retaining a smaller class where abrupt thaw should be  
304 unlikely (low ground ice).

305  
306 We assessed the ability of these ground ice maps to capture ground ice distribution at a finer scale using our thaw database. Prior  
307 to analysis, we removed abrupt thaw processes that do not require ground ice melting, ensuring that the abrupt thaw points used  
308 for this analysis only represented ice-dependent thaw processes (Table 4). We then overlaid the maps with the updated thaw  
309 database points, extracted the ground ice classification, and calculated the proportion of abrupt and non-abrupt thaw points  
310 within each ground ice class. We expected abrupt thaw points to predominantly occur in high or moderate ground ice areas and  
311 non-abrupt thaw points to occur in low to no ground ice areas. Finally, we overlaid the ice-dependent abrupt thaw points from  
312 our database with the *Database of Ice-Rich Yedoma Permafrost* by Strauss et al. (2022) and calculated the proportion of these  
313 thaw processes within the Yedoma domain. Although duplicate features were removed (section 2.1), some study sites include  
314 multiple thaw features which may result in spatial clustering of observations. Therefore, results in section 3.3 should be  
315 interpreted as representing broad regional patterns rather than statistically independent observations.

### 316 3 Results

#### 317 3.1 Database Characteristics

318 The final database contains 19,540 permafrost thaw locations spanning all ecoregions of Alaska (Fig. 1). Spatial coverage is  
319 statewide and the temporal resolution varies because the sources used to map thaw features are based on imagery spanning the  
320 past ~70 years. Of these, 18,213 points represent abrupt thaw including 10,625 thermokarst lakes, 5,463 active layer  
321 detachments, 1,450 retrogressive thaw slumps, 280 generic thermokarst processes, 209 wildfire-induced abrupt thaw features,  
322 134 thermokarst wetlands, 47 thermoerosional gullies, and 5 thaw ponds (Fig. 1). An additional 1,327 points represent non-  
323 abrupt thaw. Abrupt thaw locations were concentrated in northern Alaska (Fig. 1), reflecting the higher abundance of continuous  
324 permafrost with near-surface ground ice in this region. The classification of thaw features follows the terminology used in the  
325 source data. If the thermokarst type was not specified (i.e., fen, water track), the observation was recorded as “thermokarst” and  
326 is hereafter referred to as generic thermokarst processes. Thaw features influenced by wildfire were designated as a distinct class  
327 called “wildfire-induced thaw” and were therefore not double-counted with other categories.  
328

Deleted: 20

Deleted: 20

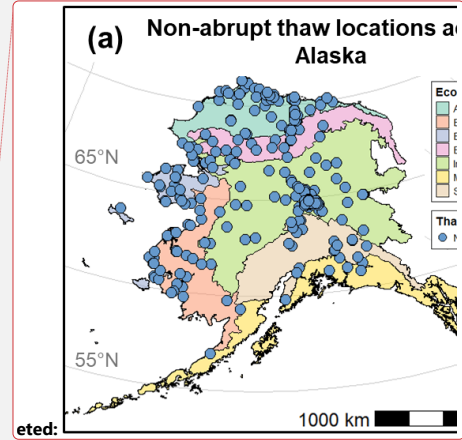
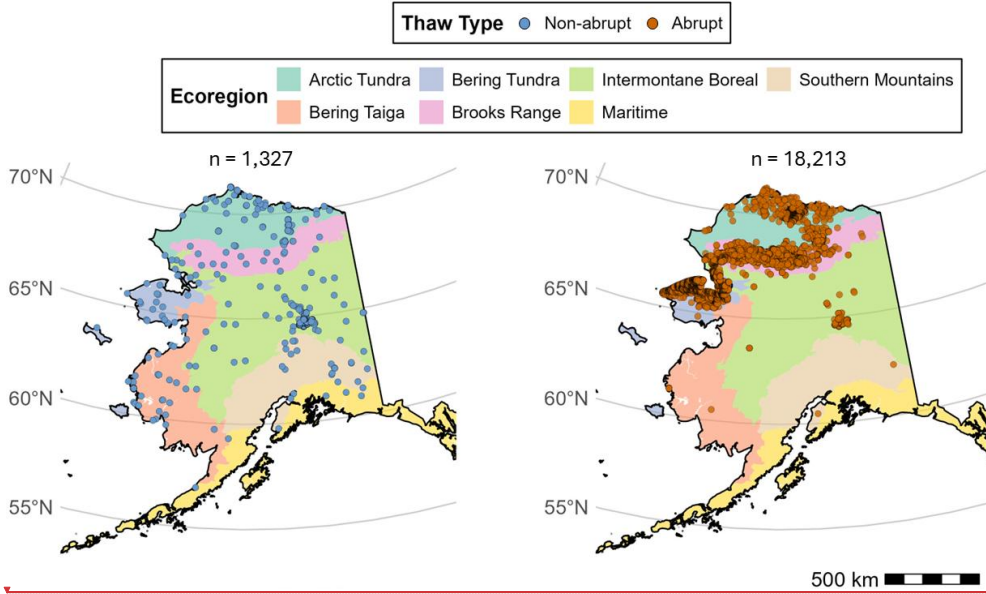
Deleted: 10 % defined as low, 10-40 % as moderate, and >40 % as high.

Deleted: 1b

Deleted: 1a

Formatted: Font: Not Bold

Formatted: Left, Indent: Left: 0", Right: 0"



335  
336 **Figure 1.** Map of non-abrupt (left) and abrupt (right) permafrost thaw locations across Alaska's ecoregions slightly modified from the Level III  
337 U.S. EPA Alaska Ecoregions Map (U.S. Environmental Protection Agency, 2012).

338 **3.2 Environmental Characteristics**

339 There were distinct regional differences in types of abrupt thaw across Alaska (Fig. 2). Active layer detachments and  
340 retrogressive thaw slumps dominated in mountainous areas like the Brooks Range, while lowland regions like the Arctic and  
341 Bering Tundra primarily experienced thermokarst lake expansion and general thermokarst activity. Abrupt thaw accounted for  
342 more than 97 % of features in the Arctic Tundra, Bering Tundra, and Brooks Range. In contrast, only 36 % of features in Interior  
343 Alaska and 17 % in the Bering Taiga were abrupt thaw while the Southern Mountains and Maritime ecoregions had virtually  
344 none. Interior Alaska exhibited the most diverse array of abrupt thaw features, with thermokarst wetlands and wildfire-driven  
345 thaw being the most common. We tested whether the distribution of abrupt thaw features differed significantly between Alaska's  
346 ecoregions using a chi-square test of independence with Monte Carlo simulation (10,000 replicates) to account for sparse data.  
347 The test revealed a highly significant association between thaw feature type and ecoregion ( $\chi^2 = 27,509$ ,  $p < 0.001$ ), indicating  
348 that abrupt thaw features are not evenly distributed across regions.  
349

Deleted: (a)

Deleted: (b)

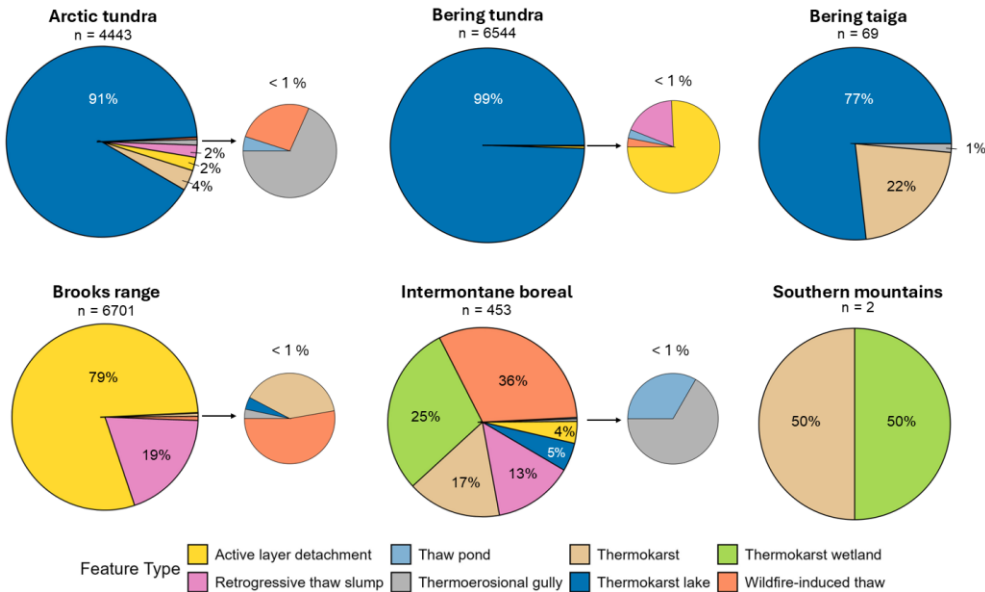
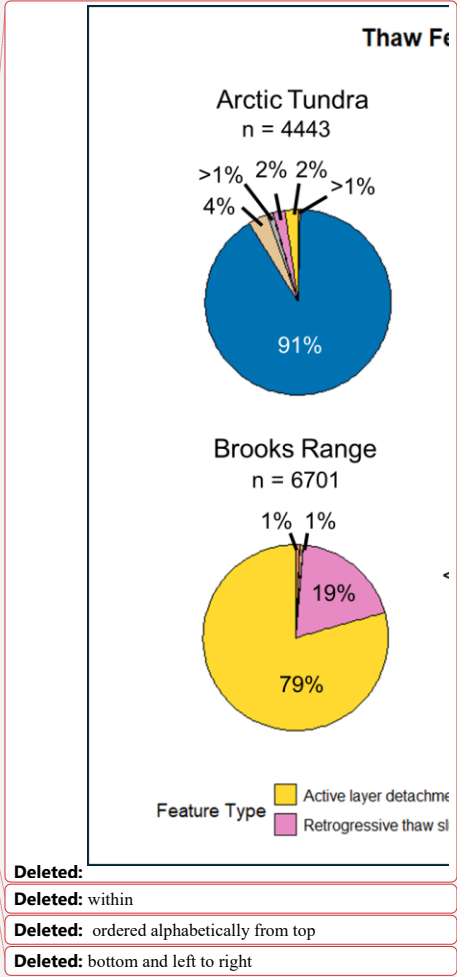


Figure 2. Proportion of abrupt thaw feature types across Alaska's major ecoregions. Smaller pie charts adjacent to each main pie highlight feature types that account for less than 1% of the total within each ecoregion. Ecoregion boundaries were adapted from the Level III U.S. EPA Alaska Ecoregions Map (U.S. Environmental Protection Agency, 2012).

Two out of three topographic variables (relative elevation and SRI) showed statistically significant differences between abrupt and non-abrupt thaw locations. Slope was not significantly different between abrupt (mean = 5.36°, 95 % CI: [4.70, 6.07]) and non-abrupt thaw locations (mean = 4.01°, 95 % CI: [3.50, 4.60]; p = 0.51). Relative elevation was significantly lower at abrupt thaw locations (mean = -0.66 m, 95 % CI: [-0.78, -0.56]) compared to non-abrupt thaw locations (mean = 0.04 m, 95 % CI: [-0.13, 0.21]; p < 0.001). Less intuitively, solar radiation index was significantly lower at abrupt thaw locations (mean = 0.71, 95 % CI: [0.70, 0.71]) compared to non-abrupt thaw locations (mean = 0.75, 95 % CI: [0.74, 0.76]; p < 0.001). Most solar radiation index values fall between 0.6 and 1 and are clustered around 0.75 because the majority of thaw features occur on flat terrain with slopes near 0 degrees. These findings suggest that abrupt thaw is more prevalent in lowlands or depressions and in areas with lower potential solar radiation (Fig. 3), while slope has no significant effect.



Deleted: within  
 Deleted: ordered alphabetically from top  
 Deleted: bottom and left to right

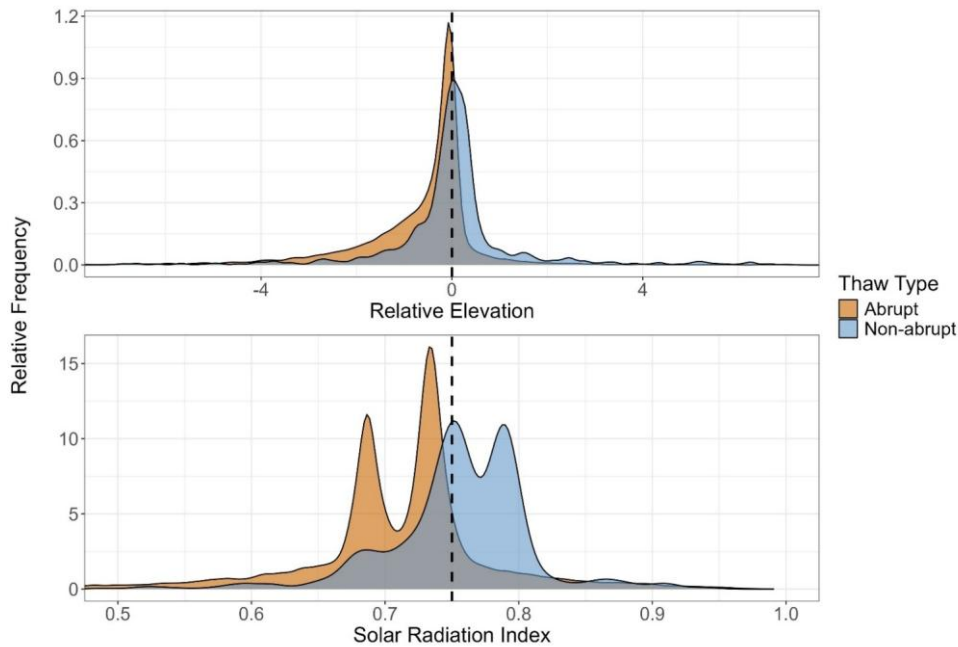
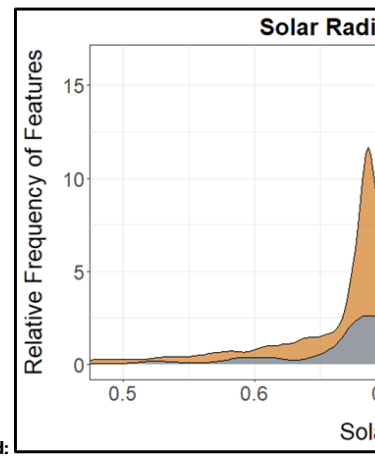
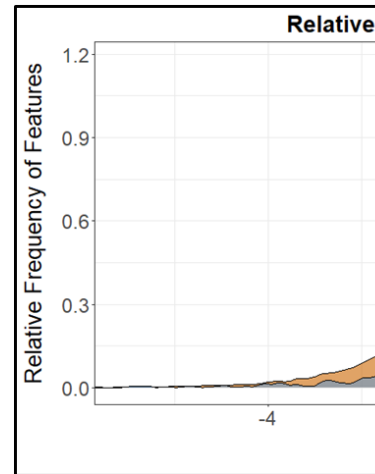


Figure 3. Distributions of relative elevation (top) and SRI (bottom) for abrupt and non-abrupt thaw locations across Alaska. In the top panel, values left of the dotted line indicate local depressions while values to the right indicate elevated terrain. In the bottom panel, the x-axis is centered at 0.75 to represent the average SRI value for flat terrain. Density curves show the relative frequency of each thaw type.

### 3.3 Spatial Comparison with Ground Ice Maps and Yedoma

When we compared our thaw database with the Jorgenson et al. (2008) ground ice map, only 65 % of ice-dependent abrupt thaw locations fell within areas classified as high or moderate ground ice while 35 % occurred in areas labeled low, variable, or unfrozen (Fig. 4). This indicates that this ground ice map only captures about two-thirds of locations where ice-dependent abrupt thaw processes actually occur, revealing a substantial mismatch between the map and observed thaw features. Spatial overlays with the Heginbottom et al. (2002) map showed that 60 % of ice-dependent abrupt thaw locations occurred in areas classified as high or moderate ground ice while 40 % were in low-ice regions (Fig. 4). The spatial distribution of ice-dependent abrupt thaw events in areas classified as having low ground ice content is not uniform across Alaska, with most of the discrepancies being in the Seward peninsula, northern tundra, and parts of interior Alaska. Because the abrupt thaw processes used in this analysis require substantial ice content to develop, these results highlight the potential limitations of existing ground ice datasets for accurately representing permafrost vulnerability at the local scale.



Deleted:

Deleted: (a)

Deleted: (b)

Deleted: (a),

Deleted: (b),

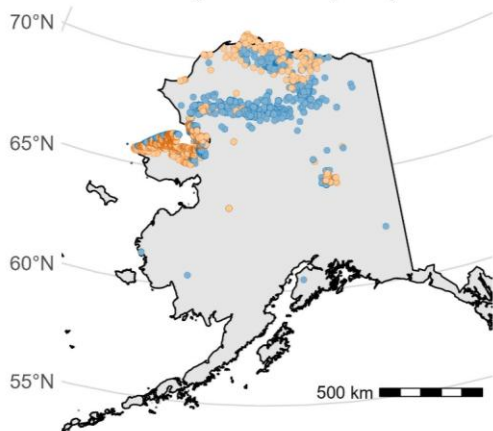
Deleted: 4a

Deleted: 4b).

Deleted: significant

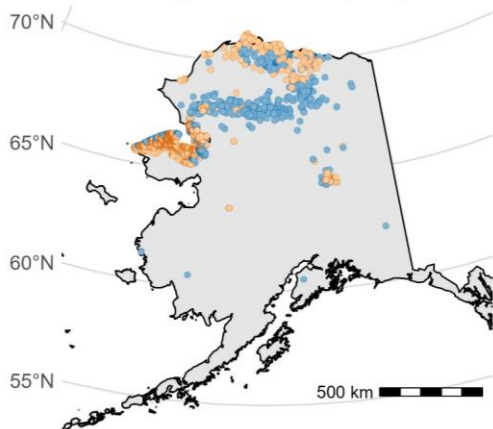
### Permafrost Characteristics of Alaska Map

Jorgenson et al. (2008)

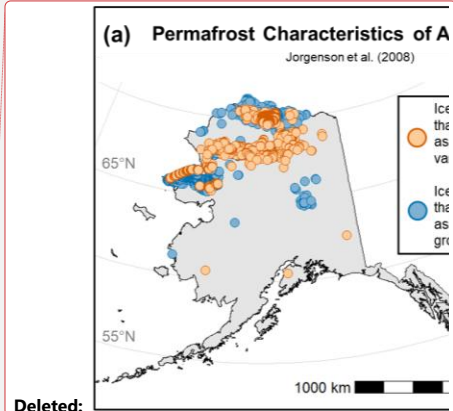


### Circum-Arctic Map of Permafrost and Ground-Ice Conditions, Version 2

Heginbottom et al. (2002)



- Ice-dependent abrupt thaw points classified as high or moderate ground ice
- Ice-dependent abrupt thaw points classified as low ground ice, variable, or unfrozen



Deleted:

Deleted: (a)

Deleted: (b)

Formatted: Font: Not Bold

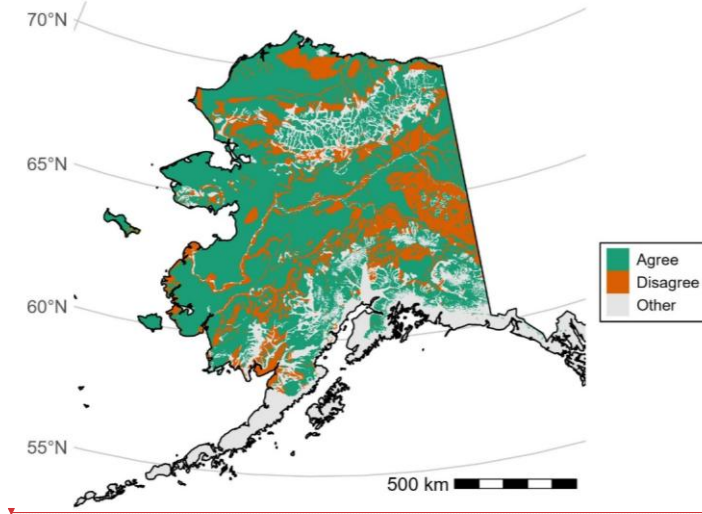
Deleted: .

**Figure 4.** Locations of potential misclassifications based on ground ice content from the *Permafrost Characteristics of Alaska* map (top) and *Circum-Arctic Map of Permafrost and Ground-Ice Conditions, Version 2* (bottom). Orange dots represent ice-dependent abrupt thaw features

396  
397  
398  
399

404 that are misclassified (i.e., mapped in areas of low, variable or unfrozen ground ice) while blue dots represent ice-dependent abrupt thaw  
405 features mapped in areas of high or moderate ground ice. [Each map shows 12,492 ice-dependent abrupt thaw features from the database.](#)  
406

407 We also examined the level of agreement between the two ground ice maps across Alaska (Fig. 5). Although Jorgenson et al.  
408 (2008) and Heginbottom et al. (2002) show comparable accuracy in identifying ice-dependent abrupt thaw features within areas  
409 classified as having high or moderate ground ice, substantial discrepancies remain in their spatial distribution of ground ice  
410 content (Fig. 5). Excluding regions without permafrost, the two maps assign the same ground ice class to only 73 % of the  
411 permafrost zone, while 27 % is classified differently, meaning that there is conflicting representation on more than one quarter of  
412 ground ice distribution in Alaska's permafrost zone. These findings suggest the maps are not only inconsistent with our fine-  
413 scale thaw database but also show considerable disagreement with each other.  
414

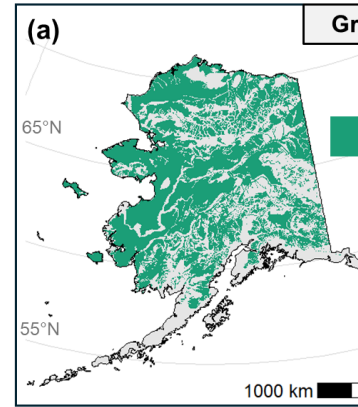


415 **Figure 5.** Map of areas where Jorgenson et al. (2008) and Heginbottom et al. (2002) agree in ground ice classification (green) and areas where  
416 the two maps disagree (orange). [Note that we combined the moderate and high classes into a single category for each map while retaining low](#)  
417 [ground ice as a distinct class.](#)  
418  
419  
420

421 In addition to evaluating ground ice maps, we examined the spatial relationship between ice-dependent abrupt thaw features (i.e.,  
422 thaw processes that require high ground ice content to form) and Yedoma. The Yedoma domain covers 38 % of Alaska, yet it  
423 includes nearly 60 % of ice-dependent abrupt thaw features from our database, indicating that a substantial proportion of these  
424 thaw processes are located in regions underlain by extremely ice- and carbon-rich permafrost (Fig. 6).  
425

**Deleted:** 5b). Notably, the two maps use different thresholds for defining ground ice classes: Jorgenson et al. (2008) classifies moderate as 10-20 % and high as >20 %, whereas Heginbottom et al. (2002) defines moderate as 10-40 % and high as > 40 %. To ensure accurate comparison between datasets, we combined the moderate and high classes into a single category for each map while retaining low ground ice as a distinct class since both maps define it as < 10 %. ...

**Formatted:** Font: 10 pt



**Deleted:**

**Deleted:** (a)

**Deleted:** blue/

**Deleted:** (b)

**Formatted:** Font: Bold

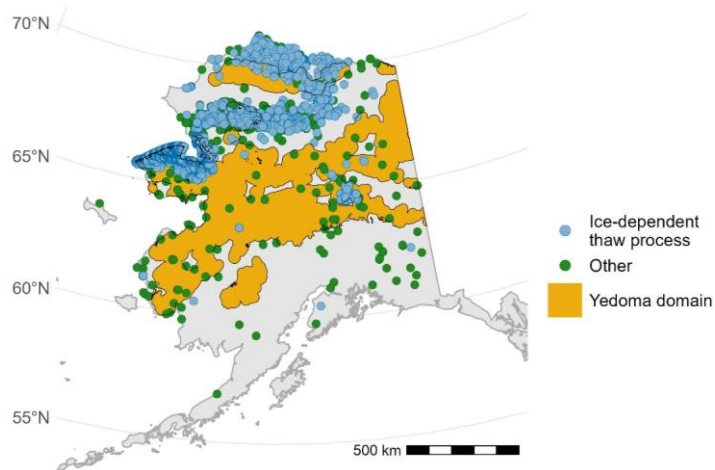
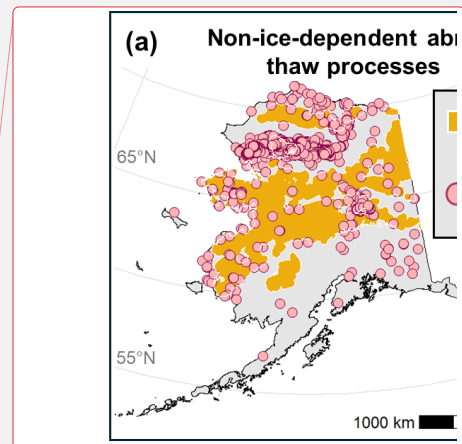


Figure 6. Map of ice-dependent (blue) abrupt thaw processes and either ice-independent abrupt thaw processes or gradual thaw processes (green) that occur within or outside the mapped Yedoma domain (yellow) according to Strauss et al. (2022).



Deleted:

Deleted: (a) non-ice-independent (pink) and (b) ice-

Deleted: gold with white outline

#### 4 Discussion

Our topographic analysis indicates that abrupt thaw is disproportionately concentrated in local depressions and valley bottoms, suggesting that these low-lying areas may serve as hotspots for abrupt thaw processes. Lowlands often experience greater aeolian or fluvial deposition of fine sediments and more peatland development which are conditions that favor high ground ice content and, over longer timescales, Yedoma formation, both of which increase thaw susceptibility. This finding aligns with previous studies showing that poor drainage in lowlands can promote permafrost degradation (Kokelj and Jorgenson, 2013; Natali et al., 2015; Schuur and Mack, 2018). We found that both relative elevation and SRI were significantly lower at abrupt thaw sites compared to non-abrupt thaw sites. One possible explanation for the higher SRI values for non-abrupt thaw features is that south-facing slopes may have a reduced capacity to accumulate and preserve large amounts of ground ice due to warmer air and soil temperatures from increased solar radiation, leading to drier, better-drained soils that are less prone to ice development and subsequent thermokarst processes. Steep slopes and high gradient areas typically have lower ground ice and shallower depth to bedrock permafrost which will not exhibit thaw features (Van Soest et al., 2025). In contrast, low SRI sites such as north-facing slopes or valley bottoms have cooler, wetter conditions conducive to ice formation, making them more susceptible to abrupt thaw once thaw initializes. It is also important to note that our SRI metric does not incorporate canopy cover or low-lying vegetation which can limit the amount of sunlight that reaches the ground surface. Dense vegetation cover in low-SRI areas could further protect ice-rich permafrost and lead to more accumulation of ground ice over time, ultimately increasing the risk of eventual ground subsidence. We observed no significant relationship between slope steepness and thaw type (abrupt vs. non-abrupt), suggesting that slope alone is not a primary control on abrupt thaw and reinforcing the need to consider multiple environmental variables such as vegetation, local hydrology, storm events, and soil temperature when assessing thaw risk.

Deleted: Slopes

Although current ground ice datasets, such as Jorgenson et al. (2008) and Heginbottom et al. (2002), are valuable for regional to pan-Arctic scale assessments, they were not designed to capture fine-scale (i.e., 10s to 100s of meters) heterogeneity in ground ice conditions that represent typical thaw feature sizes. The spatial clustering of apparent misclassifications suggests that localized ice-rich deposits may not always be resolved in regional maps. These discrepancies may rise from sub-grid heterogeneity, including ice-wedge polygon terrain, or from thermokarst legacy landscapes where thaw features formed when ground ice content was higher in the past. Our analysis revealed that only 60-65 % of abrupt thaw locations fall within areas classified as high or moderate ground ice, suggesting that current datasets may have limitations in quantifying the distribution of ice-rich permafrost at finer scales. Of these ice-dependent abrupt thaw processes, more than half (~ 59 %) occur within the mapped Yedoma domain (which only occupies 38 % of our study area) and are exceptionally ice-rich and contain large stores of organic carbon. Thaw in these regions could drive rapid ground subsidence and release vast amounts of bioavailable carbon (Strauss et al., 2017), including methane which is about 28.5 times more potent as a greenhouse gas than carbon dioxide over a 100-year time period (Bäck et al., 2024). Outside the Yedoma domain, this vulnerability is generally concentrated in the upper ~

478 3 m of permafrost as deeper gravels or bedrock tend to slow down vertical thaw feature expansion. The presence of abrupt thaw  
479 outside mapped ice-rich zones underscores the limited utility of existing maps for local-scale prediction and highlights the urgent  
480 need for higher-resolution ground ice products across Alaska and the broader Arctic to improve modeling accuracy and risk  
481 assessment for abrupt thaw. Recent efforts to explicitly map permafrost vulnerability, such as the fine-scale study of three  
482 military training lands in [interior Alaska](#) by Jorgenson et al. (2025), demonstrate the potential of integrating soil thermal  
483 conditions and permafrost characteristics into vulnerability frameworks. These detailed assessments are regional in scope, but  
484 our statewide thaw database provides an observational foundation for extending these approaches to broader landscapes.  
485 Together, these complementary efforts can create a path towards more accurate representations of permafrost thaw risk.  
486

**Deleted:** the U.S. Army Fort Wainwright

487 Our database of 19,540 features represents the most comprehensive compilation of permafrost thaw observations across Alaska.  
488 However, there are a few limitations. Spatial coverage is uneven, with denser sampling along road systems, at long term field  
489 sites, and in more accessible regions, highlighting the need for observations in underrepresented areas. There are three regions in  
490 particular that would benefit from more field observations: 1) the Northwestern Arctic Slope uplands including the Colville  
491 River drainage and the northern foothills of the Brooks Range; 2) Western Interior Alaska including much of Denali National  
492 Park and sections of the Yukon River drainage; and 3) Eastern Alaska including the northeastern Brooks Range, eastern Interior,  
493 and northeastern Alaska Range. The majority of these regions have no road access and are some of the most remote parts of  
494 Alaska; however, they comprise a large area of the state and should be prioritized in future field campaigns because additional  
495 data from these areas would improve the representativeness of the database. [Because observations in our database are not](#)  
496 [randomly sampled, the results of our statistical tests should be interpreted with caution. Sampling is biased toward regions that](#)  
497 [have had more research activity, resulting in overrepresentation of areas including the Brooks Range, Seward Peninsula, and](#)  
498 [Arctic tundra lowlands](#). Our database is also limited by relatively few non-abrupt thaw points, largely due to observational bias  
499 since non-thawing or gradually thawing landscapes are harder to detect with remote sensing and are less frequently studied.  
500 Another limitation is the dominance of thermokarst lakes in the dataset, which could skew model outputs toward aquatic thaw  
501 processes while underrepresenting terrestrial forms of abrupt thaw. While the dataset can be filtered to focus on specific thaw  
502 features, we retained all observations to preserve flexibility for diverse research applications.  
503

**Deleted:** Abrupt permafrost thaw is a critical driver of carbon release in permafrost regions, with implications that extend far beyond local ecosystems. By exposing deep, previously frozen carbon to microbial decomposition, abrupt thaw can release substantial amounts of carbon dioxide and methane into the atmosphere. While estimates remain uncertain, some models suggest that abrupt thaw could lead to a similar climate feedback as gradual thaw by creating localized hotspots of permafrost carbon release (Turetsky et al., 2020). These processes have the potential of accelerating climate warming and further constraining global carbon budgets. ¶

504 In summary, our analyses reveal how topography both governs and is transformed by abrupt thaw, yet current ground ice maps  
505 remain too coarse for reliable local-scale prediction. Future research should build on these relationships by integrating our  
506 database with geospatial layers such as soil thermal conditions, ground ice, hydrology, vegetation, and [weather](#) data to model  
507 permafrost thaw vulnerability across Alaska. This approach would inform thaw susceptibility in regions where field observations  
508 are sparse and provide more accurate prediction of abrupt thaw at local scales. Consequently, our database provides an  
509 unprecedented resource for studying the spatial patterns of permafrost thaw in Alaska while also laying the groundwork for  
510 improved methods of modeling future thaw in a rapidly changing Arctic.

¶ Beyond climate concerns, abrupt thaw poses immediate risks to communities, infrastructure, and land management. Thaw-induced ground collapse can damage roads, pipelines, buildings, and other critical infrastructure, leading to substantial economic and safety concerns. Indigenous and local communities, developers, and the U.S. military all require accurate spatial information to anticipate and respond to permafrost thaw hazards. Our database provides a foundation for understanding where permafrost is thawing to guide mitigation, adaptation, and long-term planning strategies in a rapidly changing Arctic. ¶

**Deleted:** and offers a foundation for tackling these challenges....

## 511 5 Conclusion

**Deleted:** climate

512 Our database represents the most spatially comprehensive synthesis of abrupt and non-abrupt permafrost thaw observations  
513 across Alaska to date. Our analysis reveals key topographic and environmental drivers of thaw: abrupt thaw is more prevalent in  
514 low-elevation valley bottoms and in areas with less solar radiation potential. While current ground ice maps remain valuable for  
515 large-scale assessments, their limitations at finer resolutions emphasize the need for improved products to support local-scale  
516 planning and risk mitigation. Notably, more than half of ice-dependent abrupt thaw features in our database occur in Yedoma  
517 deposits, which are exceptionally ice- and carbon-rich, highlighting these regions as potential hotspots for greenhouse gas  
518 emissions.  
519

520 The Alaska Permafrost Thaw Database provides an open-access, collaborative framework that invites continual addition,  
521 refinement, and expansion of thaw observations and serves as a foundational tool for diverse applications. It enables researchers  
522 to identify data gaps and prioritize future field campaigns while also offering critical training and validation data for modeling  
523 and machine learning efforts. By including both abruptly thawing and more stable permafrost locations, the dataset provides the  
524 contrast needed for robust modeling of thaw vulnerability. Its utility extends to local governments, planning agencies, Indigenous  
525 communities, the U.S. military, and others seeking to develop targeted adaptation and mitigation strategies in the face of  
526 accelerating permafrost degradation. As permafrost thaw continues to reshape Arctic landscapes, high-quality, accessible spatial  
527 data such as this database will be essential for anticipating change. The Alaska Permafrost Thaw Database not only provides a  
528 baseline for ongoing monitoring and modeling but also advances collective efforts to understand, prepare for, and respond to the  
529 complex impacts of permafrost thaw in a warming world.  
530

## 531 Contributing Data

561 We welcome contributions of new abrupt or non-abrupt permafrost thaw locations across Alaska. Contributions are accepted via  
562 pull requests on the GitHub repository: [https://github.com/ArcticWebb/Alaska\\_Permafrost\\_Thaw\\_Database](https://github.com/ArcticWebb/Alaska_Permafrost_Thaw_Database). See the  
563 CONTRIBUTING.md file for detailed instructions on how to submit new thaw locations.

564 **Data Availability**

565 The Alaska Permafrost Thaw Database is publicly available at  
566 [https://github.com/ArcticWebb/Alaska\\_Permafrost\\_Thaw\\_Database](https://github.com/ArcticWebb/Alaska_Permafrost_Thaw_Database) (Webb et al., 2025b). DOI:  
567 <https://doi.org/10.5281/zenodo.16996415>

Deleted: (Webb et al., 2025b)

570 **Code Availability**

571 Our Google Earth Engine Script is publicly available at  
572 [https://github.com/ArcticWebb/Alaska\\_Permafrost\\_Thaw\\_Database/tree/main/Scripts](https://github.com/ArcticWebb/Alaska_Permafrost_Thaw_Database/tree/main/Scripts).

574 **Author contribution**

575 H.W. and M.R.T. conceived the study and methodology. H.W. compiled the database, developed the Google Earth Engine script,  
576 and conducted all analyses. E.P., T.A.D., and I.O. contributed to validation by providing feedback and suggestions on the  
577 analyses. B.W.A., W.B.B., Y.C., Y.C., J.E., E.S.E., M.L., I.H.M., J.S., K.W.A., K.W., M.A.W. contributed published data to  
578 help form this database and provided feedback and suggestions to ensure their data were represented accurately. H.W. prepared  
579 the original draft of the manuscript and all authors contributed to review and editing.

581 **Competing Interests**

582 The authors declare that they have no conflict of interest.

584 **Acknowledgements**

585 The research reported here was funded in part by the Army Research Office/Army Research Laboratory via grant #W911NF-23-  
586 1-0311 to the University of Colorado Boulder. Any errors and opinions are not those of the Army Research Office or Department  
587 of Defense and are attributable solely to the authors. This material is based upon work supported by the Broad Agency  
588 Announcement Program and the Cold Regions Research and Engineering Laboratory (ERDC-CRREL) under Contract No.  
589 W913E524C0003. I.O. and E.P. initiated permafrost terrain analysis codes with support of NSF-OPP award 1844181. T.A.D.  
590 was supported by the Strategic Environmental Research and Development Program (project RC18-1170) and the Environmental  
591 Security Technology Demonstration Program (project NH22-7408). J.S. was supported by the Virtual Institute for the Carbon  
592 Cycle (VICC, project Rapid Permafrost Thaw Carbon Trajectories - PeTCaT, funded by Schmidt Sciences).

Deleted: H.W. and M.R.T. also acknowledge funding from the U.S. Army Corps of Engineers grant #W913E524C0003.

Formatted: Font: Aptos, 11 pt

594 We would also like to acknowledge the contributions of the many scientists and research teams whose published data form the  
595 foundation of this database. In total, 44 independent sources were integrated, representing decades of work across Alaska. We  
596 thank these authors for their invaluable contributions (see Table 1 and References for full source list).

600 **References**

- 601 Abbott, B. and Jones, J.: Soil respiration, water chemistry, and soil gas data for thermokarst features and undisturbed tundra on  
602 the North Slope of Alaska, <https://doi.org/10.18739/A23T9D71C>, 2013.
- 603 Andresen, C. G., Lawrence, D. M., Wilson, C. J., McGuire, A. D., Koven, C., Schaefer, K., Jafarov, E., Peng, S., Chen, X.,  
604 Gouttevin, I., Burke, E., Chadburn, S., Ji, D., Chen, G., Hayes, D., and Zhang, W.: Soil moisture and hydrology projections of  
605 the permafrost region – a model intercomparison, *The Cryosphere*, 14, 445–459, <https://doi.org/10.5194/tc-14-445-2020>, 2020.
- 606 Bäck, H., May, R., Naidu, D. S., and Eikenberry, S.: Effect of methane mitigation on global temperature under a permafrost  
607 feedback, *Glob. Environ. Change Adv.*, 2, 100005, <https://doi.org/10.1016/j.gecadv.2024.100005>, 2024.
- 608 [Ballinger, T. J., Crawford, A., and Serreze, M. C.: NOAA Arctic Report Card 2025 : Surface Air Temperature. NOAA Tech.  
609 Rep. OAR ARC 25-02, https://doi.org/10.25923/CJ60-9S07, 2025.](https://doi.org/10.25923/CJ60-9S07)
- 610 Balsler, A. and Jorgenson, M.: Surface and Upper Permafrost Site Properties, Northern Alaska,  
611 <https://doi.org/10.18739/A2JG7M>, 2013.
- 612 Bamber, J. L., Oppenheimer, M., Kopp, R. E., Aspinall, W. P., and Cooke, R. M.: Ice sheet contributions to future sea-level rise  
613 from structured expert judgment, *Proc. Natl. Acad. Sci.*, 116, 11195–11200, <https://doi.org/10.1073/pnas.1817205116>, 2019.
- 614 Bigalke, S. and Walsh, J. E.: Future Changes of Snow in Alaska and the Arctic under Stabilized Global Warming Scenarios,  
615 *Atmosphere*, 13, 541, <https://doi.org/10.3390/atmos13040541>, 2022.
- 616 Bowden, W. B., Gooseff, M. N., Balsler, A., Green, A., Peterson, B. J., and Bradford, J.: Sediment and nutrient delivery from  
617 thermokarst features in the foothills of the North Slope, Alaska: Potential impacts on headwater stream ecosystems, *J. Geophys.  
618 Res. Biogeosciences*, 113, 2007JG000470, <https://doi.org/10.1029/2007JG000470>, 2008.
- 619 Buckeridge, K. M., Shimel, J. P., Mack, M. C., and Schurr, E.: Ecosystem nutrient cycling following thermokarst disturbance,  
620 <https://doi.org/10.18739/A2V97ZS2J>, 2013.
- 621 Buckeridge, K. M., McLaren, J. R., Mack, M. C., Schuur, E. A. G., and Schimel, J.: Missing nitrogen source during ecosystem  
622 succession within retrogressive thaw slumps in Alaska, *Environ. Res. Lett.*, 18, 065003, [https://doi.org/10.1088/1748-  
623 9326/acd0c2](https://doi.org/10.1088/1748-9326/acd0c2), 2023.
- 624 Chen, Y., Liu, A., and Cheng, X.: A dataset of thermokarst lake drainage events in northern Alaska (2000–2020),  
625 <https://doi.org/10.5281/ZENODO.4998099>, 2021a.
- 626 Chen, Y., Lara, M., Jones, B., Frost, G., and Hu, F. S.: Thermokarst acceleration in Arctic tundra driven by climate change and  
627 fire disturbance, 1950–2015, <https://doi.org/10.18739/A2610VT0G>, 2021b.
- 628 Douglas, T. A., Hiemstra, C. A., Anderson, J. E., Barbato, R. A., Bjella, K. L., Deeb, E. J., Gelvin, A. B., Nelsen, P. E.,  
629 Newman, S. D., Saari, S. P., and Wagner, A. M.: Recent degradation of interior Alaska permafrost mapped with ground surveys,  
630 geophysics, deep drilling, and repeat airborne lidar, *The Cryosphere*, 15, 3555–3575, <https://doi.org/10.5194/tc-15-3555-2021>,  
631 2021.
- 632 Edwards, M., Grosse, G., Jones, B. M., and McDowell, P.: The evolution of a thermokarst-lake landscape: Late Quaternary  
633 permafrost degradation and stabilization in interior Alaska, *Sediment. Geol.*, 340, 3–14,  
634 <https://doi.org/10.1016/j.sedgeo.2016.01.018>, 2016.
- 635 Efron, B. and Tibshirani, R. J.: *An Introduction to the Bootstrap*, Springer US, Boston, MA, [https://doi.org/10.1007/978-1-4899-  
636 4541-9](https://doi.org/10.1007/978-1-4899-4541-9), 1993.
- 637 Euskirchen, E. S., Edgar, C. W., Turetsky, M. R., Waldrop, M. P., and Harden, J. W.: Differential response of carbon fluxes to  
638 climate in three peatland ecosystems that vary in the presence and stability of permafrost: Carbon fluxes and permafrost thaw, *J.  
639 Geophys. Res. Biogeosciences*, 119, 1576–1595, <https://doi.org/10.1002/2014JG002683>, 2014.

640 Fu, P. and Rich, P. M.: A geometric solar radiation model with applications in agriculture and forestry, *Comput. Electron. Agric.*,  
641 37, 25–35, [https://doi.org/10.1016/S0168-1699\(02\)00115-1](https://doi.org/10.1016/S0168-1699(02)00115-1), 2002.

642 Gagnon, S., Fortier, D., Godin, É., and Veillette, A.: The cryostratigraphy of thermo-erosion gullies in the Canadian High Arctic  
643 demonstrates the resilience of permafrost, *The Cryosphere*, 18, 4743–4763, <https://doi.org/10.5194/tc-18-4743-2024>, 2024.

644 Gibson, C. M., Chasmer, L. E., Thompson, D. K., Quinton, W. L., Flannigan, M. D., and Olefeldt, D.: Wildfire as a major driver  
645 of recent permafrost thaw in boreal peatlands, *Nat. Commun.*, 9, 3041, <https://doi.org/10.1038/s41467-018-05457-1>, 2018.

646 Gooseff, M.: Ground temperature at and near thermokarst sites around Toolik Lake Field Station, Summer 2009–Summer 2012,  
647 <https://doi.org/10.18739/A2M89X>, 2016.

648 Gorelick, N., Hancher, M., Dixon, M., Ilyushchenko, S., Thau, D., and Moore, R.: Google Earth Engine: Planetary-scale  
649 geospatial analysis for everyone, *Remote Sens. Environ.*, 202, 18–27, <https://doi.org/10.1016/j.rse.2017.06.031>, 2017.

650 GTN-P: Global Terrestrial Network for Permafrost metadata for active layer monitoring (CALM) sites,  
651 <https://doi.org/10.1594/PANGAEA.842815>, 2015a.

652 GTN-P: Global Terrestrial Network for Permafrost metadata for permafrost boreholes (TSP),  
653 <https://doi.org/10.1594/PANGAEA.842820>, 2015b.

654 Harms, T. K., Abbott, B. W., and Jones, J. B.: Thermo-erosion gullies increase nitrogen available for hydrologic export,  
655 *Biogeochemistry*, 117, 299–311, <https://doi.org/10.1007/s10533-013-9862-0>, 2013.

656 Harris, S. A., French, H. M., Heginbottom, J. A., Johnston, G. H., Ladanyi, B., Sege, D. C., and van Everdingen, R. O.: Glossary  
657 of permafrost and related ground-ice terms, *Assoc. Comm. Geotech. Res. Natl. Res. Council. Can. Ott.*, 156, 63–64, 1988.

658 Heginbottom, J., Brown, J., Ferrians, O., and Melnikov, E. S.: Circum-Arctic Map of Permafrost and Ground-Ice Conditions,  
659 Version 2, <https://doi.org/10.7265/SKBG-KF16>, 2002.

660 Hinkel, K. M., Sheng, Y., Lenters, J. D., Lyons, E. A., Beck, R. A., Eisner, W. R., and Wang, J.: Thermokarst Lakes on the  
661 Arctic Coastal Plain of Alaska: Geomorphic Controls on Bathymetry, *Permafrost. Periglac. Process.*, 23, 218–230,  
662 <https://doi.org/10.1002/ppp.1744>, 2012.

663 Hjort, J., Streletskiy, D., Doré, G., Wu, Q., Bjella, K., and Luoto, M.: Impacts of permafrost degradation on infrastructure, *Nat.*  
664 *Rev. Earth Environ.*, 3, 24–38, <https://doi.org/10.1038/s43017-021-00247-8>, 2022.

665 Hopkins, D. M.: Thaw Lakes and Thaw Sinks in the Imuruk Lake Area, Seward Peninsula, Alaska, *J. Geol.*, 57, 119–131, 1949.

666 Johnston, C. E., Ewing, S. A., Harden, J. W., Varner, R. K., Wickland, K. P., Koch, J. C., Fuller, C. C., Manies, K., and  
667 Jorgenson, M. T.: Effect of permafrost thaw on CO<sub>2</sub> and CH<sub>4</sub> exchange in a western Alaska peatland chronosequence, *Environ.*  
668 *Res. Lett.*, 9, 085004, <https://doi.org/10.1088/1748-9326/9/8/085004>, 2014.

669 Jones, B. and Zuck, C. A.: Fish Creek Watershed Lake Classification, NPRA, Alaska, 2016, <https://doi.org/10.5066/F7H70CXB>,  
670 2016.

671 Jones, B., Arp, C., Grosse, G., Nitze, I., Lara, M., Whitman, M., Farquharson, L., Kanevskiy, M., Parsekian, A., Breen, A.,  
672 Ohara, N., Rangel, R., and Hinkel, K.: Historic Lake Drainage on the Western Arctic Coastal Plain in Northern Alaska from  
673 Remote Sensing Datasets, 1955–2017, <https://doi.org/10.18739/A2DR2P85H>, 2019.

674 Jones, B. M., Baughman, C. A., Romanovsky, V. E., Parsekian, A. D., Babcock, E. L., Stephani, E., Jones, M. C., Grosse, G.,  
675 and Berg, E. E.: Presence of rapidly degrading permafrost plateaus in south-central Alaska, *The Cryosphere*, 10, 2673–2692,  
676 <https://doi.org/10.5194/tc-10-2673-2016>, 2016.

677 Jones, B. M., Schaeffer Tessier, S., Tessier, T., Brubaker, M., Brook, M., Schaeffer, J., Ward Jones, M. K., Grosse, G., Nitze, I.,  
678 Rettelbach, T., Zavoico, S., Clark, J. A., and Tape, K. D.: Integrating local environmental observations and remote sensing to  
679 better understand the life cycle of a thermokarst lake in Arctic Alaska, *Arct. Antarct. Alp. Res.*, 55, 2195518,  
680 <https://doi.org/10.1080/15230430.2023.2195518>, 2023.

681 Jones, M. C., Booth, R. K., Yu, Z., and Ferry, P.: A 2200-Year Record of Permafrost Dynamics and Carbon Cycling in a  
682 Collapse-Scar Bog, Interior Alaska, *Ecosystems*, 16, 1–19, <https://doi.org/10.1007/s10021-012-9592-5>, 2013.

683 Jongejans, L. L., Strauss, J., Lenz, J., Peterse, F., Mangelsdorf, K., Fuchs, M., and Grosse, G.: Table S1: Sedimentological and  
684 biogeochemical data of yedoma and thermokarst deposits in Baldwin Peninsula, West-Alaska,  
685 <https://doi.org/10.1594/PANGAEA.892306>, 2018.

686 Jorgenson, M., Yoshikawa, K., Kanevskiy, M., Shur, Y., Romanovsky, V., Marchenko, S., Grosse, G., Brown, J., and Jones, B.:  
687 Permafrost characteristics of Alaska, 2008.

688 Jorgenson, M. T., Shur, Y. L., and Pullman, E. R.: Abrupt increase in permafrost degradation in Arctic Alaska, *Geophys. Res.  
689 Lett.*, 33, L02503, <https://doi.org/10.1029/2005GL024960>, 2006.

690 Jorgenson, M. T., Brown, D. R. N., Hiemstra, C. A., Genet, H., Marcot, B. G., Murphy, R. J., and Douglas, T. A.: Drivers of  
691 historical and projected changes in diverse boreal ecosystems: fires, thermokarst, riverine dynamics, and humans, *Environ. Res.  
692 Lett.*, 17, 045016, <https://doi.org/10.1088/1748-9326/ac5c0d>, 2022.

693 Jorgenson, M. T., Douglas, T. A., Shur, Y. L., and Kanevskiy, M. Z.: Mapping the Vulnerability of Boreal Permafrost in Central  
694 Alaska in Relation to Thaw Rate, Ground Ice, and Thermokarst Development, *J. Geophys. Res. Earth Surf.*, 130,  
695 e2024JF008030, <https://doi.org/10.1029/2024JF008030>, 2025.

696 Jorgenson, T.: Permafrost soil database with information on site, topography, geomorphology, hydrology, soil stratigraphy, soil  
697 carbon, ground ice isotopes, and vegetation at thermokarst features near Toolik and Noatak River, 2009-2013,  
698 <https://doi.org/10.18739/A2CP5C>, 2013.

699 Kallio, A. and Rieger, S.: Recession of Permafrost in a Cultivated Soil of Interior Alaska, *Soil Sci. Soc. Am. J.*, 33, 430–432,  
700 <https://doi.org/10.2136/sssaj1969.03615995003300030028x>, 1969.

701 Karjalainen, O., Aalto, J., Kanevskiy, M. Z., Luoto, M., and Hjort, J.: Ground ice content predictions for the Northern  
702 Hemisphere permafrost region at 1-km resolution, version 1.1 (Version 1.1), <https://doi.org/10.5281/ZENODO.7009875>, 2022.

703 Klein, E. S., Yu, Z., and Booth, R. K.: Recent increase in peatland carbon accumulation in a thermokarst lake basin in  
704 southwestern Alaska, *Palaeogeogr. Palaeoclimatol. Palaeoecol.*, 392, 186–195, <https://doi.org/10.1016/j.palaeo.2013.09.009>,  
705 2013.

706 Kokelj, S. V. and Jorgenson, M. T.: Advances in Thermokarst Research, *Permafr. Periglac. Process.*, 24, 108–119,  
707 <https://doi.org/10.1002/ppp.1779>, 2013.

708 Kreig, R. A. and Reger, R. D.: Air-photo analysis and summary of landform soil properties along the route of the trans-Alaska  
709 pipeline system, Alaska Division of Geological & Geophysical Surveys, <https://doi.org/10.14509/426>, 1982.

710 Langer, M., Kaiser, S., Oehme, A., and Jacobi, S.: Bathymetry data of thermokarst lakes in the North Slope of Alaska (USA) and  
711 Manitoba (Canada) in 2019, <https://doi.org/10.1594/PANGAEA.918918>, 2020.

712 Lenz, J., Jones, B. M., Wetterich, S., Tjallingii, R., Fritz, M., Arp, C. D., Rudaya, N., and Grosse, G.: Bulk sediment parameter  
713 of three sediment cores from permafrost lowlands, Alaska Arctic Coastal Plain, <https://doi.org/10.1594/PANGAEA.864814>,  
714 2016.

715 Lewkowicz, A., Wolfe, S., Geological Survey of Canada, Roujanski, V., Tetra Tech Canada, Hoeve, E., HoeveEng Consulting  
716 Ltd, O'Neill, B., Geological Survey of Canada, Gruber, S., Carleton University, Roy-Léveillé, P., Université Laval, Brown, N.,  
717 Carleton University, Koenig, C., BGC Engineering, Brooks, H., BGC Engineering, Rudy, A., Northwest Territories Geological  
718 Survey, Bonnaventure, P., University of Lethbridge, Paquette, M., and Stantec: An Illustrated Permafrost Dictionary, Canadian  
719 Permafrost Association (CPA), <https://doi.org/10.52381/CPA.permafrostdictionary.1>, 2024.

720 Li, B., Heijmans, M. M. P. D., Blok, D., Wang, P., Karsanaev, S. V., Maximov, T. C., Van Huissteden, J., and Berendse, F.:  
721 Thaw pond development and initial vegetation succession in experimental plots at a Siberian lowland tundra site, *Plant Soil*, 420,  
722 147–162, <https://doi.org/10.1007/s11104-017-3369-8>, 2017.

- 723 Liljedahl, A., Hinzman, L., Busey, R., and Yoshikawa, K.: Physical short-term changes after a tussock tundra fire, Seward  
724 Peninsula, Alaska, *J. Geophys. Res. Earth Surf.*, 112, 2006JF000554, <https://doi.org/10.1029/2006JF000554>, 2007.
- 725 Lloyd, A. H., Yoshikawa, K., Fastie, C. L., Hinzman, L., and Fraver, M.: Effects of permafrost degradation on woody vegetation  
726 at arctic treeline on the Seward Peninsula, Alaska, *Permafrost. Periglac. Process.*, 14, 93–101, <https://doi.org/10.1002/ppp.446>,  
727 2003.
- 728 Luken, J. O. and Billings, W. D.: Changes in Bryophyte Production Associated with a Thermokarst Erosion Cycle in a Subarctic  
729 Bog, *Lindbergia*, 9, 163–168, 1984.
- 730 Mackelprang, R., Saleska, S. R., Jacobsen, C. S., Jansson, J. K., and Taş, N.: Permafrost Meta-Omics and Climate Change,  
731 *Annu. Rev. Earth Planet. Sci.*, 44, 439–462, <https://doi.org/10.1146/annurev-earth-060614-105126>, 2016.
- 732 McCarty, J. L., Aalto, J., Paunu, V.-V., Arnold, S. R., Eckhardt, S., Klimont, Z., Fain, J. J., Evangeliou, N., Venäläinen, A.,  
733 Tchekakova, N. M., Parfenova, E. I., Kupiainen, K., Soja, A. J., Huang, L., and Wilson, S.: Reviews and syntheses: Arctic fire  
734 regimes and emissions in the 21st century, *Biogeosciences*, 18, 5053–5083, <https://doi.org/10.5194/bg-18-5053-2021>, 2021.
- 735 [McKnight, P. E. and Najab, J.: Mann-Whitney U Test, in: The Corsini Encyclopedia of Psychology, edited by: Weiner, I. B. and](https://doi.org/10.1002/9780470479216.corpsy0524)  
736 [Craighead, W. E., Wiley, 1–1, https://doi.org/10.1002/9780470479216.corpsy0524, 2010.](https://doi.org/10.1002/9780470479216.corpsy0524)
- 737 Myers-Smith, I. H., McGuire, A. D., Harden, J. W., and Chapin, F. S.: Influence of disturbance on carbon exchange in a  
738 permafrost collapse and adjacent burned forest, *J. Geophys. Res. Biogeosciences*, 112, 2007JG000423,  
739 <https://doi.org/10.1029/2007JG000423>, 2007.
- 740 Myers-Smith, I. H., Harden, J. W., Wilkening, M., Fuller, C. C., McGuire, A. D., and Chapin, F. S.: Ages and isotopic signatures  
741 of peat cores from a boreal landscape, Interior Alaska, <https://doi.org/10.1594/PANGAEA.817460>, 2008.
- 742 Natali, S. M., Schuur, E. A. G., Mauritz, M., Schade, J. D., Celis, G., Crummer, K. G., Johnston, C., Krapek, J., Pegoraro, E.,  
743 Salmon, V. G., and Webb, E. E.: Permafrost thaw and soil moisture driving CO<sub>2</sub> and CH<sub>4</sub> release from upland tundra, *J.*  
744 *Geophys. Res. Biogeosciences*, 120, 525–537, <https://doi.org/10.1002/2014JG002872>, 2015.
- 745 National Snow and Ice Data Center (NSIDC): Cryosphere Glossary, n.d.
- 746 Nitze, I., Grosse, G., Jones, B. M., Romanovsky, V. E., and Boike, J.: Remote sensing quantifies widespread abundance of  
747 permafrost region disturbances across the Arctic and Subarctic, *Datasets*, <https://doi.org/10.1594/PANGAEA.894755>, 2018.
- 748 Nitze, I., Cooley, S. W., Duguay, C. R., Jones, B. M., and Grosse, G.: Spatial lake dynamics and lake-ice datasets of the  
749 Northern Seward and Baldwin Peninsulas in Alaska, <https://doi.org/10.1594/PANGAEA.922808>, 2020a.
- 750 Nitze, I., Cooley, S. W., Duguay, C. R., Jones, B. M., and Grosse, G.: The catastrophic thermokarst lake drainage events of 2018  
751 in northwestern Alaska: fast-forward into the future, *The Cryosphere*, 14, 4279–4297, <https://doi.org/10.5194/tc-14-4279-2020>,  
752 2020b.
- 753 Olefeldt, D., Goswami, S., Grosse, G., Hayes, D., Hugelius, G., Kuhry, P., McGuire, A. D., Romanovsky, V. E., Sannel, A. B.  
754 K., Schuur, E. A. G., and Turetsky, M. R.: Circumpolar distribution and carbon storage of thermokarst landscapes, *Nat.*  
755 *Commun.*, 7, 13043, <https://doi.org/10.1038/ncomms13043>, 2016.
- 756 Osterkamp, T. E., Viereck, L., Shur, Y., Jorgenson, M. T., Racine, C., Doyle, A., and Boone, R. D.: Observations of  
757 Thermokarst and Its Impact on Boreal Forests in Alaska, U.S.A., *Arct. Antarct. Alp. Res.*, 32, 303–315,  
758 <https://doi.org/10.1080/15230430.2000.12003368>, 2018.
- 759 Plug, L. J. and West, J. J.: Thaw lake expansion in a two-dimensional coupled model of heat transfer, thaw subsidence, and mass  
760 movement, *J. Geophys. Res. Earth Surf.*, 114, 2006JF000740, <https://doi.org/10.1029/2006JF000740>, 2009.
- 761 Porter, C., Howat, I., Noh, M.-J., Husby, E., Khuvis, S., Danish, E., Tomko, K., Gardiner, J., Negrete, A., Yadav, B., Klassen, J.,  
762 Kelleher, C., Cloutier, M., Bakker, J., Enos, J., Arnold, G., Bauer, G., Morin, P., and Polar Geospatial Center: ArcticDEM -  
763 Mosaics, Version 4.1 (1.0), <https://doi.org/10.7910/DVN/3VDC4W>, 2023.

764 Schuur, E. A. G. and Mack, M. C.: Ecological Response to Permafrost Thaw and Consequences for Local and Global Ecosystem  
765 Services, *Annu. Rev. Ecol. Evol. Syst.*, 49, 279–301, <https://doi.org/10.1146/annurev-ecolsys-121415-032349>, 2018.

766 Schuur, E. A. G., McGuire, A. D., Schädel, C., Grosse, G., Harden, J. W., Hayes, D. J., Hugelius, G., Koven, C. D., Kuhry, P.,  
767 Lawrence, D. M., Natali, S. M., Olefeldt, D., Romanovsky, V. E., Schaefer, K., Turetsky, M. R., Treat, C. C., and Vonk, J. E.:  
768 Climate change and the permafrost carbon feedback, *Nature*, 520, 171–179, <https://doi.org/10.1038/nature14338>, 2015.

769 Schuur, E. A. G., Abbott, B. W., Commane, R., Ernakovich, J., Euskirchen, E., Hugelius, G., Grosse, G., Jones, M., Koven, C.,  
770 Leshyk, V., Lawrence, D., Lorant, M. M., Mauritz, M., Olefeldt, D., Natali, S., Rodenhizer, H., Salmon, V., Schädel, C.,  
771 Strauss, J., Treat, C., and Turetsky, M.: Permafrost and Climate Change: Carbon Cycle Feedbacks From the Warming Arctic,  
772 *Annu. Rev. Environ. Resour.*, 47, 343–371, <https://doi.org/10.1146/annurev-environ-012220-011847>, 2022.

773 Stepien, A., Koivurova, T., Gremesperger, A., and Niemi, H.: Arctic Indigenous Peoples and the Challenge of Climate Change,  
774 in: *Arctic Marine Governance*, edited by: Tedsen, E., Cavalieri, S., and Kraemer, R. A., Springer Berlin Heidelberg, Berlin,  
775 Heidelberg, 71–99, [https://doi.org/10.1007/978-3-642-38595-7\\_4](https://doi.org/10.1007/978-3-642-38595-7_4), 2014.

776 Strauss, J., Schirmermeister, L., Grosse, G., Fortier, D., Hugelius, G., Knoblauch, C., Romanovsky, V., Schädel, C., Schneider Von  
777 Deimling, T., Schuur, E. A. G., Shmelev, D., Ulrich, M., and Veremeeva, A.: Deep Yedoma permafrost: A synthesis of  
778 depositional characteristics and carbon vulnerability, *Earth-Sci. Rev.*, 172, 75–86,  
779 <https://doi.org/10.1016/j.earscirev.2017.07.007>, 2017.

780 Strauss, J., Laboor, S., Schirmermeister, L., Fedorov, A. N., Fortier, D., Froese, D., Fuchs, M., Günther, F., Grigoriev, M., Harden,  
781 J., Hugelius, G., Jongejans, L. L., Kanevskiy, M., Kholodov, A., Kunitsky, V., Kraev, G., Lozhkin, A., Rivkina, E., Shur, Y.,  
782 Siegert, C., Spektor, V., Streletskaia, I., Ulrich, M., Vartanyan, S., Veremeeva, A., Anthony, K. W., Wetterich, S., Zimov, N.,  
783 and Grosse, G.: Circum-Arctic Map of the Yedoma Permafrost Domain, *Front. Earth Sci.*, 9, 758360,  
784 <https://doi.org/10.3389/feart.2021.758360>, 2021.

785 Strauss, J., Laboor, S., Schirmermeister, L., Fedorov, A. N., Fortier, D., Froese, D. G., Fuchs, M., Günther, F., Grigoriev, M. N.,  
786 Harden, J. W., Hugelius, G., Jongejans, L. L., Kanevskiy, M. Z., Kholodov, A. L., Kunitsky, V., Kraev, G., Lozhkin, A. V.,  
787 Rivkina, E., Shur, Y., Siegert, C., Spektor, V., Streletskaia, I., Ulrich, M., Vartanyan, S. L., Veremeeva, A., Walter Anthony, K.  
788 M., Wetterich, S., Zimov, N. S., and Grosse, G.: Database of Ice-Rich Yedoma Permafrost Version 2 (IRYP v2),  
789 <https://doi.org/10.1594/PANGAEA.940078>, 2022.

790 Strauss, J., Fuchs, M., Hugelius, G., Miesner, F., Nitze, I., Opfergelt, S., Schuur, E., Treat, C., Turetsky, M., Yang, Y., and  
791 Grosse, G.: Organic matter storage and vulnerability in the permafrost domain, in: *Encyclopedia of Quaternary Science*, Elsevier,  
792 399–410, <https://doi.org/10.1016/B978-0-323-99931-1.00164-1>, 2025.

793 Streletskiy, D. A., Clemens, S., Lanckman, J.-P., and Shiklomanov, N. I.: The costs of Arctic infrastructure damages due to  
794 permafrost degradation, *Environ. Res. Lett.*, 18, 015006, <https://doi.org/10.1088/1748-9326/acab18>, 2023.

795 Swanson, D. K.: Permafrost thaw-related slope failures in Alaska’s Arctic National Parks, 1980–2019., *Permafr. Periglac.*  
796 *Process.*, 32, 392–406, <https://doi.org/10.1002/ppp.2098>, 2021.

797 Teufel, B. and Sushama, L.: Abrupt changes across the Arctic permafrost region endanger northern development, *Nat. Clim.*  
798 *Change*, 9, 858–862, <https://doi.org/10.1038/s41558-019-0614-6>, 2019.

799 Turetsky, M. R., Abbott, B. W., Jones, M. C., Walter Anthony, K., Olefeldt, D., Schuur, E. A. G., Koven, C., McGuire, A. D.,  
800 Grosse, G., Kuhry, P., Hugelius, G., Lawrence, D. M., Gibson, C., and Sannel, A. B. K.: Permafrost collapse is accelerating  
801 carbon release, *Nature*, 569, 32–34, <https://doi.org/10.1038/d41586-019-01313-4>, 2019.

802 Turetsky, M. R., Abbott, B. W., Jones, M. C., Anthony, K. W., Olefeldt, D., Schuur, E. A. G., Grosse, G., Kuhry, P., Hugelius,  
803 G., Koven, C., Lawrence, D. M., Gibson, C., Sannel, A. B. K., and McGuire, A. D.: Carbon release through abrupt permafrost  
804 thaw, *Nat. Geosci.*, 13, 138–143, <https://doi.org/10.1038/s41561-019-0526-0>, 2020.

805 U.S. Environmental Protection Agency: Level III Ecoregions of Alaska, 2012.

806 Van Soest, M. A. J., Anderson, N. J., and Bullard, J. E.: Arctic soil development under changing climate conditions, *CATENA*,  
807 254, 108938, <https://doi.org/10.1016/j.catena.2025.108938>, 2025.

**Deleted:** Raftery, A. E., Zimmer, A., Frierson, D. M. W., Startz, R., and Liu, P.: Less than 2 °C warming by 2100 unlikely, *Nat. Clim. Change*, 7, 637–641, <https://doi.org/10.1038/nclimate3352>, 2017.¶  
Rantanen, M., Karpechko, A. Yu., Lipponen, A., Nordling, K., Hyvärinen, O., Ruosteenoja, K., Vihma, T., and Laaksonen, A.: The Arctic has warmed nearly four times faster than the globe since 1979, *Commun. Earth Environ.*, 3, 168, <https://doi.org/10.1038/s43247-022-00498-3>, 2022.¶

817 Vincent, W. F.: Arctic Climate Change: Local Impacts, Global Consequences, and Policy Implications, in: The Palgrave  
818 Handbook of Arctic Policy and Politics, edited by: Coates, K. S. and Holroyd, C., Springer International Publishing, Cham, 507–  
819 526, [https://doi.org/10.1007/978-3-030-20557-7\\_31](https://doi.org/10.1007/978-3-030-20557-7_31), 2020.

820 Walter Anthony, K.: Methane ebullition hotspot point data locations in interior Alaska thermokarst lakes from April 2011  
821 through October 2019, <https://doi.org/10.18739/A2NP1WK35>, 2020.

822 Wang, K., Overeem, I., Jafarov, E., Clow, G., Romanovsky, V., Schaefer, K., Urban, F., Cable, W., Piper, M., Schwalm, C.,  
823 Zhang, T., Kholodov, A., Sousanes, P., Loso, M., Swanson, D., and Hill, K.: A synthesis dataset of near-surface permafrost  
824 conditions for Alaska, 1997-2016, <https://doi.org/10.18739/A2KG55>, 2018a.

825 Wang, K., Jafarov, E., Overeem, I., Romanovsky, V., Schaefer, K., Clow, G., Urban, F., Cable, W., Piper, M., Schwalm, C.,  
826 Zhang, T., Kholodov, A., Sousanes, P., Loso, M., and Hill, K.: A synthesis dataset of permafrost-affected soil thermal conditions  
827 for Alaska, USA, *Earth Syst. Sci. Data*, 10, 2311–2328, <https://doi.org/10.5194/essd-10-2311-2018>, 2018b.

828 Webb, H., Fuchs, M., Abbott, B. W., Douglas, T. A., Elder, C. D., Ernakovich, J. G., Euskirchen, E. S., Göckede, M., Grosse, G.,  
829 Hugelius, G., Jones, M. C., Koven, C., Kropp, H., Lathrop, E., Li, W., Lorant, M. M., Natali, S. M., Olefeldt, D., Schädel, C.,  
830 Schuur, E. A. G., Sonntag, O., Strauss, J., Virkkala, A.-M., and Turetsky, M. R.: A Review of Abrupt Permafrost Thaw:  
831 Definitions, Usage, and a Proposed Conceptual Framework, *Curr. Clim. Change Rep.*, 11, 7, <https://doi.org/10.1007/s40641-025-00204-3>, 2025a.

833 Webb, H., Pierce, E., Abbott, B. A., Bowden, W. B., Chen, Y., Chen, Y., Douglas, T. A., Eklof, J. F., Euskirchen, E., Jones, M.  
834 C., Langer, M., Myers-Smith, I. H., Overeem, I., Strauss, J., Walter Anthony, K., Wang, K., Whitley, M. A., and Turetsky, M.:  
835 The Alaska Permafrost Thaw Database (Version 2.0.0), <https://doi.org/10.5281/ZENODO.16996415>, 2025b.

836 Wendel, J.: Map Reveals Hot Spots for Arctic Greenhouse Gas Emissions, *Eos*, 97, <https://doi.org/10.1029/2016EO061233>,  
837 2016.

838 Whitley, M., Frost, G. V., Jorgenson, M. T., Macander, M. J., Maio, C. V., and Winder, S. G.: Arctic-Boreal Vulnerability  
839 Experiment (ABOVE)ABOVE: Permafrost Measurements and Distribution Across the Y-K Delta, Alaska, 2016,  
840 <https://doi.org/10.3334/ORNLDAAAC/1598>, 1 January 2018.

841 Witharana, C., Udawalpola, M. R., Liljedahl, A. K., Jones, M. K. W., Jones, B. M., Hasan, A., Joshi, D., and Manos, E.:  
842 Automated Detection of Retrogressive Thaw Slumps in the High Arctic Using High-Resolution Satellite Imagery, *Remote Sens.*,  
843 14, 4132, <https://doi.org/10.3390/rs14174132>, 2022.

844 Yang, Y., Rogers, B. M., Fiske, G., Watts, J., Potter, S., Windholz, T., Mullen, A., Nitze, I., and Natali, S. M.: Mapping  
845 retrogressive thaw slumps using deep neural networks, *Remote Sens. Environ.*, 288, 113495,  
846 <https://doi.org/10.1016/j.rse.2023.113495>, 2023.

847 Yang, Y., Rodenhizer, H., Rogers, B. M., Dean, J., Singh, R., Windholz, T., Poston, A., Potter, S., Zolkos, S., Fiske, G., Watts,  
848 J., Huang, L., Witharana, C., Nitze, I., Nesterova, N., Barth, S., Grosse, G., Lantz, T., Runge, A., Lombardo, L., Nicu, I. C.,  
849 Rubensdotter, L., Makopoulou, E., and Natali, S.: A Collaborative and Scalable Geospatial Data Set for Arctic Retrogressive  
850 Thaw Slumps with Data Standards, *Sci. Data*, 12, 18, <https://doi.org/10.1038/s41597-025-04372-7>, 2025.

851 Yoshikawa, K., Bolton, W. R., Romanovsky, V. E., Fukuda, M., and Hinzman, L. D.: Impacts of wildfire on the permafrost in  
852 the boreal forests of Interior Alaska, *J. Geophys. Res. Atmospheres*, 107, <https://doi.org/10.1029/2001JD000438>, 2002.

853